creative commons
COMMONS DEED

저작자표시-비영리-변경금지 2.0 대한민국

이용자는 아래의 조건을 따르는 경우에 한하여 자유롭게

- 이 저작물을 복제, 배포, 전송, 전시, 공연 및 방송할 수 있습니다.

다음과 같은 조건을 따라야 합니다:

저작자표시. 귀하는 원저작자를 표시하여야 합니다.

비영리. 귀하는 이 저작물을 영리 목적으로 이용할 수 없습니다.

변경금지. 귀하는 이 저작물을 개작, 변형 또는 가공할 수 없습니다.

- 귀하는, 이 저작물의 재이용이나 배포의 경우, 이 저작물에 적용된 이용허락조건을 명확하게 나타내어야 합니다.
- 저작권자로부터 별도의 허가를 받으면 이러한 조건들은 적용되지 않습니다.

저작권법에 따른 이용자의 권리는 위의 내용에 의하여 영향을 받지 않습니다.

이것은 이용허락규약(Legal Code)을 이해하기 쉽게 요약한 것입니다.

Disclaimer

dCollection

이학박사학위논문

MAP kinase 신호전달계의 피드백 조절 기작과 속도 결정 단계 연구

Feedback regulation mechanisms and the rate-determining step of the yeast MAP kinase pathway

2016 년 8 월

서울대학교 대학원

생명과학부

최 민 연

Feedback regulation mechanisms and the rate-determining step of the yeast MAP kinase pathway

By

Min-Yeon Choi

Advisor

Professor Sang-Hyun Park, Ph.D.

A Thesis for the Degree of Doctor of Philosophy

August, 2016

School of Biological Sciences

Seoul National University

ABSTRACT

Feedback regulation mechanisms and the rate-determining step of the yeast MAP kinase pathway

Min-Yeon Choi

School of Biological Sciences

Seoul National University

Three-tier module of the MAP kinase pathway is a classical type of signal transduction system well-known for regulating cell functions in response to diverse external stimuli. MAP kinase pathways exist in all types of eukaryotes with its vast number of components and connections to control cell's fate. For such complex system to function properly within the seemingly chaotic cellular environment, MAP kinase pathway must be tightly regulated for a reliable signal transmission. Many of the key components, participating proteins, and their interacting network have been identified. However, we know far less about the core structure (connections) that controls the three-tier module. MAP kinase pathway is tightly regulated for a reliable signal transmission and ultimately decision making of the cell. In this study, we explored the rate-determining step and the core control circuit by combining experimental results, mathematical modeling and comparison between the two.

To experimentally identify the rate-determining step of the MAP kinase pathway, we used kinases from the yeast mating pathway as a model. We manipulated abundances of three key players of the yeast mating pathway. The three kinases form the three-tier that is sequentially activated and therefore essential to

the signal transmission of the mating pathway. We modified protein abundance by under-expression and over-expression of each kinase and observed how the overall signal transduction is affected. Previously, reducing protein expression is mainly limited by the difficulties associated with controlling the reduction level and in some cases the initial endogenous abundance is too low. For the under-expression to be useful as an experimental tool, repeatability and stability of reduced expression is important. We found that *cis*-elements in programmed −1 ribosomal frameshifting (−1RFS) of beet western yellow virus (BWYV) could be utilized to reduced protein expression in *Saccharomyces cerevisiae*. The two main advantages of using −1RFS are adjustable reduction rates and ease of use. Programmed −1RFS was used for under-expression whereas over-expression was achieved with stronger promoter and high-copy plasmids. Three kinases were subjected to six variations of abundance differing from their endogenous expression levels. The results showed that signal output decreased as Ste11 abundance decreased and the output increased as the abundance of Ste11 increased, identifying ste11 as the rate-determining component.

We have developed a novel mathematical model of the yeast mating pathway to investigate how ste11, MAPKKK, alone affects the overall outcome and to find the rate-determining step and the controlling regulation mechanisms of the yeast decision making system. We constructed a three component model with all possible connections which comes to a total of 2187 structures. 2187 structures went through multiple analyses including elimination process, fitness analysis, and synergy analysis to yield a core structure that represents the yeast mating pathway. The optimal structure revealed that at least two negative feedbacks and a positive feedback are needed as a regulation mechanism to explain the rate-determining effects of ste11 and robustness of Ste7 and Fus3. Positive feedback can be explained with increased output strength in a constitutively active ste11 mimicking amplification taking place between ste11 and ste7. Addition to multiple negative regulations already known from previous studies, we identify new negative regulations on ste7 by Ppq1 which seems to be activated by Fus3. Combination of

these regulations facilitates the three component signal transduction system for a controlled and robust response.

Cells also face randomness of life with equally complex orchestration of internal stochasticity and controlled stability. Cell-to-cell variations, even in an isogenic population are inevitable and increasing evidence suggests that cells can strategically limit the noise but also benefit from the variation caused by the noise. However, origins, characteristics and significance of these variations are partially known and remain controversial. Here, we track MAP kinase signaling pathway responses of yeast single cells and quantitatively analyze each response profiles to find the existence of response profile stochasticity (RPS). We find that response profiles of isogenic yeast populations are distinct enough to be divided into groups that differed in response speed and duration. Interestingly, RPS is an inherent trait that increases diversity as an individual by allowing different responses every time while maintaining a consistent and robust average response as a population. Our findings indicate that yeast cells increase survival chance at both population and individual levels with RPS originating from the MAP kinase signaling pathway by diversifying under identical genetic and environment backgrounds.

Keywords: Feedback regulation, Protein abundance, Rate-determining step, Response profile, *Saccharomyces cerevisiae*, Stochasticity
Student number: 2009-30859

COPYRIGHT INFORMATION

Portions of this dissertation have appeared in separate publication:

Min-Yeon Choi and Sang-Hyun Park. Adjustable under-expression of yeast mating pathway proteins in Saccharomyces cerevisiae using a programmed ribosomal frameshift. Appl Microbiol Biotechnol (2016) 100:4997−5005.

TABLE OF CONTENTS

LIST OF FIGURES

LIST OF TABLES

ABBREVIATIONS

−1RFS	programmed −1 ribosomal frameshifting
BWYV	beet western yellow virus
DIC	differential interference contrasts
EGFP	enhanced green fluorescent protein
FACS	fluorescence-activated cell sorting
fluc	firefly luciferase
HA	Human influenza hemagglutinin
LC-MS/MS	liquid chromatography tandem mass spectrometry
MAPKKK	mitogen-activated protein kinase kinase kinase
MAPKK	mitogen-activated protein kinase kinase
MAPK	mitogen-activated protein kinase
PCR	polymerase chain reaction
PPQ	protein phosphatase q
RPS	response profile stochasticity
Ser	serine
SDS-PAGE	sodium dodecyl sulfate polyacrylamide gel electrophoresis
SRP	signal response profile
Thr	threonine
Tyr	tyrosine
yEGFP	yeast enhanced green fluorescent protein

CHAPTER 1. Adjustable under-expression of yeast mating pathway proteins in *Saccharomyces cerevisiae* using a programmed ribosomal frameshift

INTRODUCTION

An important part of studying molecular and cellular biology is the identification of a gene and its functions[1]. Because gene expression is among the most fundamental levels at which a cell controls its phenotype, studies of gene function often begin by eliminating gene expression. This gene deletion can interrupt related cellular processes, and phenotypic comparison analyses with non-deleted type can elucidate the functions of the gene in question. Upregulation of gene expression and subsequent observation of the effects comprise another study method. Yeast, a good model organism, can be easily manipulated by deleting or over-expressing a gene of choice[2-4]. Despite the long histories of these methods, which have served us well and made great contributions to the advancement of biology, disadvantages and limitations remain. In some cases, gene deletion can be lethal, whereas in other cases, deletion or over-expression is not sufficient to fully understand the true endogenous functions[5, 6]. Furthermore, studies expanding to the identification of complex and dynamic gene regulatory networks, that could include amplification, inhibition, compensation, and feedback regulation, require expression methods that are more fine-tuned than deletion or over-expression.

The aim of this study was developing a method of gene under-expression at various protein abundance levels using ribosomal frameshifting. Programmed translational frameshifting is commonly used by viruses to allow the synthesis of two distinctive proteins from a single mRNA[7]. In this experiment, a frameshift element from the beet western yellow virus (BWYV) was used to reduce protein expression levels of targeted yeast mating pathway components in a repeatable and stable fashion. The BWYV frameshift element consists of a slippery sequence and a RNA pseudoknot sequence connected by a 6-codon spacer sequence that has been well defined by studies of frameshift rate control. During −1 ribosomal frameshifting (−1RFS), mRNA sequences are alternatively translated by moving the tRNA in the −1 direction at the designated slippery sequence with a predetermined frequency. According to previous studies, the stability and integrity of frameshifting

efficiency depends on the relatively small and tightly folded RNA structure of the RNA pseudoknot which allows a stable and significant production of the −1 frameshift[8, 9]. Accordingly, the −1RFS is ideal for experiments as point mutations and insertions in its sequence can alter the rate of frameshifting, thereby, giving us the ability to control protein expression to the required levels. Furthermore, this technique is inexpensive, easily implemented and the reduction rate can be readily adjusted. Along with deletion and over-expression, a well-established under-expression technique could become experimentally useful as a tool in the studies of *S. cerevisiae*.

Here, we subjected yeast mating pathway components, including the Ste5 scaffold protein, Ste11, Ste7, and Fus3, to under-expression. We then applied −1RFS constructs to Fus3, a MAPK of the yeast signaling pathway, to determine how the application of protein under-expression would influence signal transduction. MAP kinase pathways are chains of proteins that transmit signals from receptors on the surface to the DNAs in the nucleus, that are found to have complex regulation mechanisms along with reports of noise in gene expressions[10, 11]. Therefore, given the fluctuating gene expression, signaling pathways are likely to be influenced by the expression levels of their components and are thus interesting subjects for the application of under-expression. Fus3 regulates many different signal transduction outputs critical for the mating of haploid yeast cells[12-14]. To analyze the contribution of Fus3 abundance to the signal output, we measured the changes in Fus3 activation and Fus1 transcription in response to Fus3 under-expression.

MATERIALS AND METHODS

Yeast strains, plasmids and growth conditions

W303 (ATCC208352) served as the background strain for all *S. cerevisiae* strains used in this study. RB210 (*MAT***a**, *mfa::Fus1-LacZ, fus3::URA3, kss1::Kan*^{R}), SH152 (*MAT***a**, *mfa::Fus1-LacZ, ste7::URA3, kss1:: Kan*^{R}), SH153 (SO992 *MAT***a**, *mfa::Fus1-LacZ, ste11::URA3, kss1::Kan*^{R}) and RB207 (*MAT***a**, *mfa::Fus1-LacZ, ste5::LEU2, kss1::Kan*^{R}) were generated via PCR-based gene deletion using pFA6a-GFP(65T)-URA3 as a template[15, 16].

The frameshift element (fs) sequence from BWYV used in this experiment is TTTAAAC-TAGTTG-CGCGGCACCGTCCGCGGAACAAACGGGC, consisting of slippery-space-pseudoknot sequence. All of the plasmids used for the luciferase assay experiments have an endogenous promoter, frameshift element, gene of interest, and firefly luciferase (fluc) in sequence as an insert. Expression level tests were performed using fluc-tagged *Fus3* constructs, which were generated by transforming RB210 cells with pRS314-Fus3-fluc (*CEN/ARS*, ampR, TRP1), pRS314-fs-Fus3-fluc (*CEN/ARS*, ampR, TRP1), or pRS314-fs-inFus3-fluc (*CEN/ARS*, ampR, TRP1). To test the expression levels of fluc-tagged *Ste11* constructs, SH153 cells were transformed with pRS314-fs-Ste11-fluc (*CEN/ARS*, ampR, TRP1) or pRS314-fs-inSte11-fluc (*CEN/ARS*, ampR, TRP1). To test the expression level of fluc-tagged *Ste7* constructs, SH152 cells were transformed with pRS314-fs-Ste7-fluc (*CEN/ARS*, ampR, TRP1) or pRS314-fs-inSte7-fluc (*CEN/ARS*, ampR, TRP1). For the expression level test of fluc-tagged *Ste5* constructs, RB207 cells were transformed with pRS314-fs-Ste5-fluc (*CEN/ARS*, ampR, TRP1) or pRS314-fs-inSte5-fluc (*CEN/ARS*, ampR, TRP1). Additionally, pRS316-pFus1-EGFP (Frameshift *CEN/ARS*, ampR, URA3) was used to detect pFus1 transcription levels for a signal transduction readout. To detect the endogenous expression levels of *Fus3*, *Ste11*, *Ste7*, and S*te5*, fluc was chromosomally integrated to the 3′-end of endogenous *Fus3*, *Ste11*, *Ste7*, or *Ste5*, respectively in RB206 (*MAT***a**, *mfa::Fus1-*

LacZ, kss1::Kan^{R}), resulting in four different strains in which each respective gene was tagged with fluc. For the signal transduction test, the same constructs without the fluc tags were used.

Yeast cells were grown at 30°C in a shaking incubator at 200 rpm and in a selective media. 2% Dextrose (w/v) was used as a carbon source. A peptide corresponding to the mating pheromone, α-factor, was chemically synthesized using fluorenylmethoxycarbonyl (F-moc) chemistry and purified via high-performance liquid chromatography (HPLC).

Luciferase reporter assay

Cells in the exponential growth phase were harvested and lysed by vortexing with acid-washed glass beads (Sigma-Aldrich, St. Louis, MO, USA) in Y-PER lysis solution (Thermo Fisher Scientific, Rockford, IL, USA) containing a protease inhibitor cocktail (Sigma-Aldrich) and phosphatase inhibitor cocktails (Sigma-Aldrich). To control for variations in protein concentrations, the samples were subjected to a Bradford assay (Bio-Rad, Hercules, CA, USA) using bovine serum albumin (BSA) as a standard prior to the luciferase assay. Luciferase assays were performed using the Luciferase assay system (Promega, Madison, WI, USA) in which 20 μl/well of cleared lysate and 100 μl of luciferase assay reagent were added to a well of a 96-well plate. The resulting production of light was measured with a luminometer (LB9501, Berthold, Bad Wildbad, Germany) following the manufacturer's protocol. Transformation of each construct was performed in triplicates and the resulting data are presented as average values from three assays performed on three separate days. Luciferase activities are expressed as means ± standard deviations.

Cell preparation and fluorescence-activated cell sorting (FACS)

Cells grown in overnight culture were diluted to an OD_{600} of 0.2 in SD-TRP

medium with 2% dextrose (w/v) as a carbon source and grown to mid-log phase (OD_{600} = 0.5). For FACS analysis of pFus1-EGFP expression, 300 μl of individual cell cultures were transferred to 5-ml tubes and sonicated for 3 s to separate cell clumps. Subsequently, 10,000 cells per sample were analyzed using a flow cytometer (FACSCanto; BD Biosciences, San Jose, CA, USA). Cells were treated with α-factor at a final concentration of 1 μM for up to 2 h to trigger the mating signal. Time point 0 denotes pre-stimulation time point and 30, 60, 90, and 120 min represent the time intervals after stimulation. All transfected cell populations were 100% viable based on forward and side-scatter parameters. Three independent experiments were performed in triplicates.

Cell lysis and western blot analysis

500-ml cell cultures were grown to log phase and then treated with α-factor at a final concentration of 1 μM to trigger mating response. Next, 50-ml aliquots of the cultures were harvested at various time points (0, 15, 30, 90 min) and frozen in liquid nitrogen. The cells were lysed using glass beads in a Y-PER (Thermo Fisher Scientific) lysis solution containing protease and phosphatase inhibitors (Sigma-Aldrich). The soluble fraction was separated from the cell debris by two-step centrifugations at 16,000 *g* for 10 min at 4℃. The concentrations of total proteins in the cleared lysates were measured using a Bradford Assay kit (Bio-Rad). The protein mixtures were separated by 10% sodium dodecyl sulfatepolyacrylamide gel electrophoresis (SDS-PAGE) and transferred to nitrocellulose membranes (Whatman, Dassel, Germany). The membranes were blocked with 1% skim milk in Tris-buffered saline with 1% Tween-20 (TBST) for 1 h at room temperature and then incubated with the appropriate primary antibody for 1 h to overnight at 4℃. The following primary antibodies were used in this study: anti-Fus3 (yN-19; Santa Cruz Biotechnology, Dallas, TX, USA) and anti-phospho-p44/42 (9101; Cell Signaling Technology, Danvers, MA, USA). After an overnight incubation with the appropriate primary antibody, each membrane were washed several times with

TBST and then incubated with a horseradish peroxidase-conjugated anti-goat (Santa Cruz Biotechnology, Dallas, TX, USA) or anti-rabbit (Cell Signaling Technology, Danvers, MA, USA) secondary antibody as appropriate. The proteins were detected with an LAS-3000 imaging system (Fujifilm, Tokyo, Japan) and West Pico chemiluminescent substrate (Thermo Fisher Scientific).

Halo assay

A lawn of cells was treated with pheromone at a localized source to determine the extent of cell growth inhibition. A small amount of subject yeast strain from a fresh colony was inoculated in YPD and grown overnight. Next, a sterilized 0.5% agar solution was mixed with a small volume of saturated starter culture and poured onto an appropriate solid media. A paper disk containing α-factor was then placed in the middle of the plate and the plate was incubated at 30°C until a lawn of cells appeared[17]. The result of halo assay indicates a zone of growth inhibition surrounding the filter soaked with pheromone.

RESULTS

Template constructs for the −1 frameshifting element

The BWYV frameshift elements used in this experiment is composed of slippery, spacer and pseudoknot sequences[8, 18]. A frameshift element was inserted between the flag-tag and start codon of Fus3. The basic concept of frameshift under-expression is the production of functional Fus3 in response to the occurrence of −1 frameshifting at the slippery sequence before the Fus3 initiation codon, thus enabling translation through Fus3, which sits in the −1 frame. If a frameshift does not occur, translation stops at the TAG stop codon within the spacer sequence only producing flag-tag (Fig. 1a). Three representative constructs were made by mutating the wild-type BWYV −1RFS frameshift element to demonstrate how this element can be manipulated to express various levels of protein. The first construct (fs_1) was designed by inserting a single A after CCGCGG in the middle of the pseudoknot sequence. The second construct (fs_2) had a point mutation from CCGCGG to CCGCGT and an insertion of A changing the middle of the pseudoknot sequence to CCGCGTA. The third construct (fs_3) contained a different spacer sequence, ATGCAT, which did not have a stop codon and had the same mutation as the second construct but with an inserted C codon instead of A. The in-frame construct (in frame) featured the exact same sequence as the third construct but has an additional A at the end of the pseudoknot sequence to move the previously −1 positioned Fus3 in frame. In this case, the in frame translation produced a functional Fus3, whereas the −1 frameshift produced a very short protein with no activity (Fig. 1b).

Protein abundance was detected linearly using the luciferase assay

A luciferase assay based linearity test was performed to verify the dynamic range for the optimal detection of under-expressed proteins. First, the whole cell lysate

Figure 1.

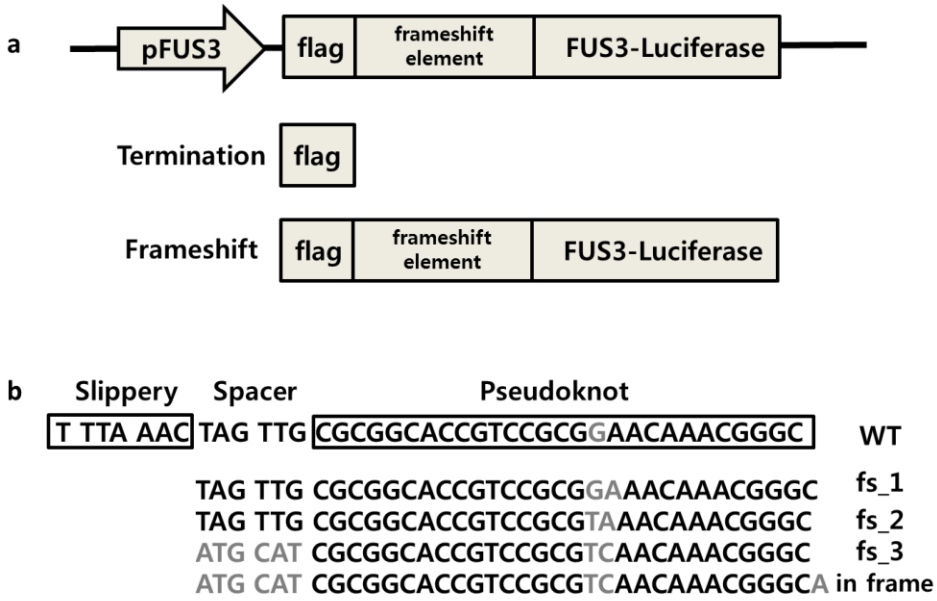
a
pFUS3
flag
frameshift element
FUS3-Luciferase
Termination
flag
Frameshift
flag
frameshift element
FUS3-Luciferase
b
Slippery
Spacer
Pseudoknot
T TTA AAC TAG TTG CGCGGCACCGTCCGCGGAACAAACGGGC WT
TAG TTG CGCGGCACCGTCCGCGGAAACAAACGGGC fs_1
TAG TTG CGCGGCACCGTCCGCGTAAACAAACGGGC fs_2
ATG CAT CGCGGCACCGTCCGCGTCAACAAACGGGC fs_3
ATG CAT CGCGGCACCGTCCGCGTCAACAAACGGGCA in frame

Figure 1. Concept of under-expression by programmed -1 ribosomal frameshifting (-1RFS).

(a) Schematic representation describing how a programmed frameshift element controls protein abundance. A stop sequence exists within the frameshift element. If a frameshift does not occur, translation is terminated after the flag. Luciferase fused Fus3 is produced only if a −1 frameshift occurs. (b) Sequence of the BWYV frameshift element consisting of slippery, spacer and pseudoknot regions. The −1 frameshifting occurs in the slippery region and the spacer contains a stop codon. Four sequences of mutated BWYV frameshift elements used in this experiment are shown along with the wild-type sequence. Fs_1 contains an insertion (A), fs_2 contains a single mutation (G to T) and an insertion (A) in the pseudoknot region, fs_3 contains a different spacer sequence (ATG CAT) along with a mutation (G to T) and an insertion (C) in the pseudoknot region, and the in frame construct has the same sequence as fs_3 but with an additional insertion (A) at the end of the pseudoknot region.

concentration was calibrated with a Bradford assay. Then, the lysates were diluted with lysis buffer to yield cell lysate solutions with total protein concentrations ranging from 0.01 μg to 5 μg. Finally, the various concentrations of Fus3 protein in the whole-cell lysates were measured using the luciferase reporter assay described in the Materials and Methods. The results showed a linear increase in Fus3 abundance as the total protein concentration increased, verifying that the whole-cell lysate concentration as measured by the Bradford assay accordingly represented the increasing concentration of Fus3. Therefore, the luciferase assay accurately reflected increases and decreases in the concentration of fluc-tagged Fus3. Protein concentrations of Fus3 were detected in the range exceeding 500 folds (Fig. 2a).

BWYV frameshift elements decrease expression level of yeast proteins

To better understand the effect of BWYV −1 frameshift elements on the yeast translational system, we aimed to express Fus3 of the yeast mating pathway at 20%−50% of the endogenous level using a selection of three frameshift constructs. We used the luciferase reporter assay system to quantitatively measure the abundances of under-expressed proteins (Fig. 1b). The first construct contained an extra codon A inserted in the pseudoknot region (fs_1), the second construct had a G to U mutation and an extra codon A in the pseudoknot region (fs_2), and the third construct contained a G to U mutation and an extra codon C in the pseudoknot region (fs_3). Relative to the endogenous Fus3 expression level, which was set at 100, the three constructs expressed 28.0%, 42.4%, and 44.8%, respectively (Fig. 2b). In a previous study with virus, the same constructs had frameshift rates of 10.5%, 23.6%, and 30.5%, respectively, in vitro[9]. Although the exact rates of occurrence differed between virus and yeast, the same patterns of mutational effects were observed at an increased frameshift rate. The yeast translational mechanism appears to broadly mirror the viral frameshift efficiency pattern, but with an enhanced frameshift rate relative to the rates observed in the virus.

Figure 2.

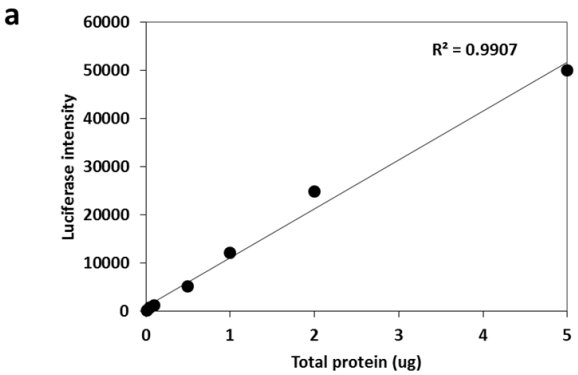

Total protein (μg)	Luciferase intensity
0.01	241
0.05	758
0.1	1224
0.5	5280
1	12231
2	24837
5	50117

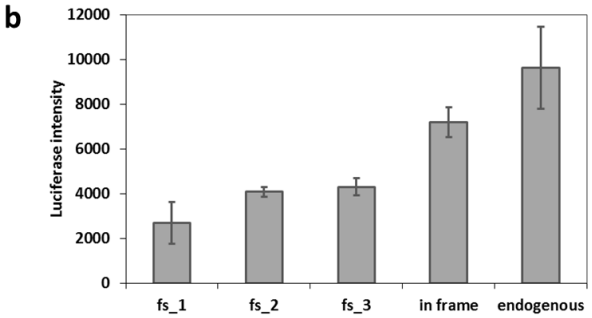

Constructs	Protein expression (%)
fs_1	28.0
fs_2	42.4
fs_3	44.8
in frame	74.8
endogenous	100

Figure 2. Protein expression intensity as measured via luciferase assay.

(a) Linearity and dynamic range of the luciferase assay. The luciferase intensity increases linearly as the total protein concentration increases. Seven different concentrations were diluted from a total cell lysate and measured to verify the dynamic range of the assay. (b) Detection of Fus3 abundance via luciferase assay. The graph presents the Fus3 abundance levels resulting from three frameshift constructs with different mutated sequences, an in frame construct and the endogenous construct. The graph shows the actual detection intensity, and the numbers in the side table represent the Fus3 expression levels from each construct relative to the endogenous Fus3 expression in the wild-type yeast. Values in the graph represent the means and standard deviations from three separate experiments.

To confirm the frameshifting function and rates in vivo, other components of the yeast mating pathway including Ste11, Ste7, and Ste5 were also subjected to under-expression. All three proteins were expressed with their own promoters; therefore, the frameshift efficiencies were compared to each of their own endogenous abundance. The fs_2 construct was used for the under-expression verification and comparison with other four mating pathway components, Ste5, Ste11, Ste7 and Fus3. The results showed that the frameshift constructs reduced abundances of all members of the mating MAP kinase pathway relative to the endogenous abundance levels. When the four different signaling components were subjected to under-expression, the protein levels ranged between 11% and 50% of the wild-type (Fig. 3).

BWYV −1 frameshift elements can be manipulated to be in in-frame to achieve more diverse protein abundance

Frameshift constructs shown so far operated by placing the start codon of Fus3 in a −1 frame so that the functional protein was translated only when a −1 frameshift occurs, and translation proceeds through the frameshift element and Fus3. Therefore, −1 frameshifting efficiency equaled the abundance of Fus3 made. However, even with various insertion or mutations in the pseudoknot sequence, the highest achievable frameshift rate was approximately 30% in the virus, corresponding to roughly 50% in yeast. To obtain protein abundance rates between 50% and 100% of the endogenous expression level, we reversed the concept of the −1 frameshift so that Fus3 sits in in-frame and the spacer sequence did not have a stop codon. In this case, a functional protein was translated when −1 frameshifting did not occur. On the other hand, if −1 frameshift did occur, only 11 amino acids of Fus3 would be translated, which is too short to have any functional effect on the mating pathway. We used the fs_3 construct and added an A codon at the end of the pseudoknot sequence immediately before the Fus3 start codon to create the in frame construct.

Figure 3.

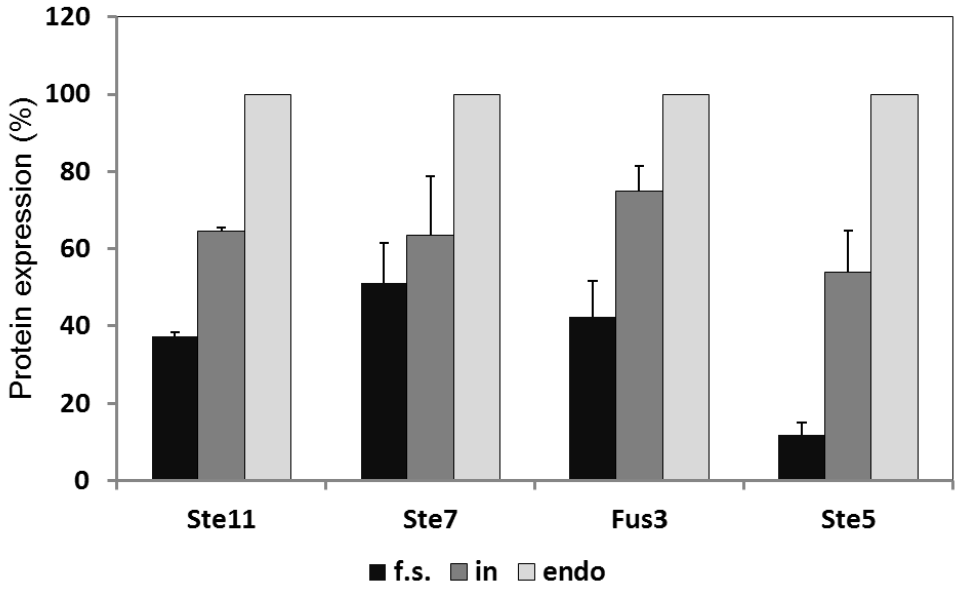
120
100
80
60
40
20
0
Protein expression (%)
Ste11
Ste7
Fus3
Ste5
f.s.
in
endo

Figure 3. Protein Expression levels of yeast mating pathway proteins as detected via luciferase assay.

The expression levels of Ste11, Ste7, Fus3, and Ste5 are presented as percentages relative to the corresponding endogenous levels in wild-type yeast. Values in the graph represent the means and standard deviations from three separate experiments. F.s., frameshift construct_2; in, in frame construct.

The addition of a codon in this position placed the previously −1 frame positioned Fus3 in frame. Because we used average of 45% yielding fs_3 construct to make the in frame construct, we expected the in frame construct to produce a yield higher than 55%. In the luciferase assay, Fus3-fluc with the in frame construct produced a 75% Fus3 expression rate relative to the endogenous abundance (Fig. 2b). This in frame concept was applied to Ste11, Ste7, and Ste5 to achieve expression rates of 64%, 63% and 54%, respectively (Fig. 3). These results verify that the in frame construct can also be used for a stable under-expression.

MAP kinase pathway signal output can be manipulated by the under-expression of MAPK, Fus3

The mating signal flows through the yeast MAP kinase pathway to activate pheromone responsive genes that induce cell cycle arrest and changes in cellular morphology, resulting in the making of shmoo for fusion with a partner cell (Fig. 4a). The dually phosphorylated Fus3 MAPK, the final kinase of the yeast mating pathway, regulates many different signal transduction outputs that govern the ability of *S. cerevisiae* haploid cells to mate[13, 19, 20]. We observed how Fus3 under-expression influences the signal pathway output, beginning with the activation of Fus3, which leads to the induction of Fus1 and then to the level of cell cycle arrest. Fus3 was under-expressed at multiple levels and compared with the wild-type to determine its effects on signal transduction in the mating pathway at different output levels. The fs_2 and in frame constructs were used for under-expression, which yielded approximate expression rates of 42% and 75%, respectively, compared to the endogenous abundance of Fus3.

The under-expression of Fus3 was also verified by Fus3 immunoblotting and a time course immunoblotting revealed a decrease in Fus3 activation, detected by measuring Fus3 dual phosphorylation, as Fus3 expression level decreased (Fig. 4b top). The maximum activation level was achieved at the wild-type abundance, and a stepwise decrease in Fus3 abundance resulted in an abundance dependent

decrease in the activation level. A previous study reported that only less than 20% of the existing Fus3 proteins are dually phosphorylated, whereas about 50% remain unphosphorylated[13]. Combined with the well-known fact that Fus3 is induced upon pheromone stimulation, it was interesting to observe that a gradual decrease in Fus3 abundance led to a gradual decrease in the Fus3 activation level, despite the low rate of activation observed with the wildtype.

To determine how these decreases in Fus3 protein abundance and activation rates would affect the induction of a mating related gene, we measured pFus1-EGFP expression over a 120 minutes time course. Flow cytometry measuring pheromone-induced pFus1-EGFP revealed reductions in both speed and magnitude as the Fus3 abundance decreased (Fig. 4b bottom). Since low Fus3 abundance decreased the sensitivity of gene expression in response to pheromone stimulation, we wanted to determine whether such difference would be sufficient to change the cell's responsiveness. To detect pheromone responsiveness in Fus3 under-expressed cells, we performed a halo assay, a type of growth inhibition plate assay. The halo assay was performed with wildtype cells (100% Fus3 expression) and fs_2 construct bearing cells (42% expression) to observe the greatest difference. This comparison revealed a significant reduction in the resulting growth inhibition zone, or halo, surrounding the 42% expressing cells (Fig. 4c).

Together, these results showed that the manipulation of a single signaling component could decrease the self-activation rate, thus decreasing the overall signal amplitude and sensitivity to stimulus, without altering the stimulus strength. In addition, by reducing the Fus3 abundance, we determined that the endogenous Fus3 expression level could not be compensated and that the natural abundance is critical for the maximal output of the mating signal.

Figure 4.

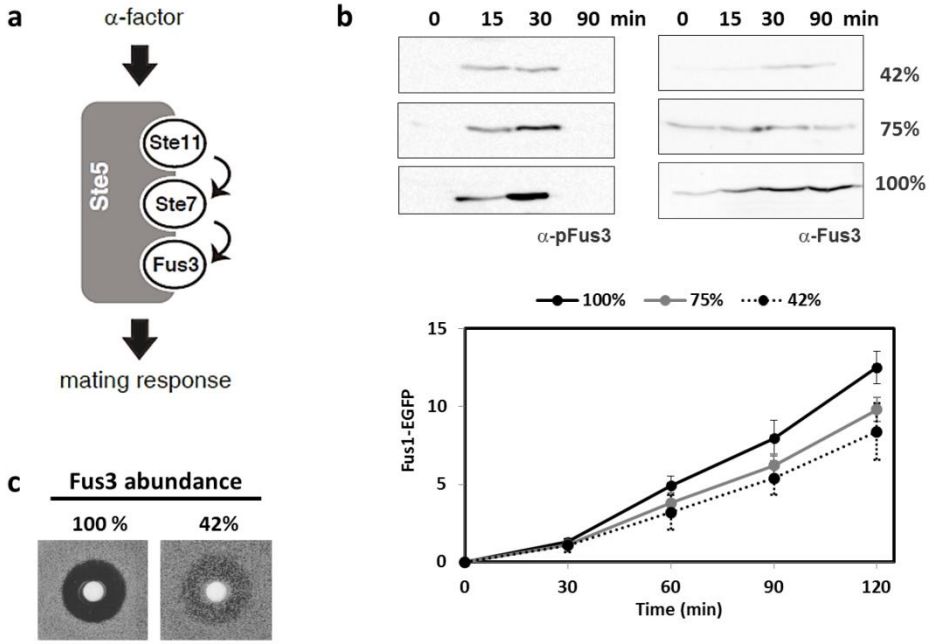
a
α-factor
Ste5
Ste11
Ste7
Fus3
mating response
b
0 15 30 90 min
0 15 30 90 min
42%
75%
100%
α-pFus3
α-Fus3
100% 75% 42%
Fus1-EGFP
15
10
5
0
0 30 60 90 120
Time (min)
c
Fus3 abundance
100 %
42%

Figure 4. Overall effects of Fus3 under-expression on signal transduction in the yeast mating pathway.

(a) Representation of the yeast mating MAP kinase pathway. The pheromone α-factor initiates pathway, which stimulates the MAPK signaling cascade consisting of Ste5 scaffold protein and the kinases Ste11, Ste7, and Fus3. The signal flows through the MAP kinase pathway to activate the pheromone responsive genes, resulting in the mating response. (b) Top: Yeast cultures in the late exponential growth phase were treated with α-factor at a final concentration of 1 μM. Cells were harvested before treatment and at 15 min, 30 min and 90 min after treatment. Proteins were separated by SDS-PAGE and subjected to Western blotting analysis. Fus3 proteins were detected by anti-Fus3 antibody, and Fus3 activity was determined with an anti-pFus3 antibody. Bottom: Yeast cultures in the late exponential growth phase were treated with α-factor at a final concentration of 1 μM. Green fluorescence was detected before the treatment and at every 30 min after treatment, with a final time point at 120 min. Each dot represents the means and standard errors of the mean (n = 3). The value of 100% represents endogenous abundance, whereas 75% represents Fus3 abundance from the in frame construct and 42% represents Fus3 abundance from the frameshift_2 construct. (c) The mating halo assay involving cells with different Fus3 expression levels. Here, 100% Fus3 abundance corresponds to the endogenous expression level and 42% indicates the under-expressed abundance resulting from frameshifting with fs_2. Representative results of multiple trials (n = 3) are shown.

DISCUSSION

Yeast has been a popular model organism due to its easy genetic accessibility as many experiments in molecular biology incorporate over-expression and deletion to study genes and their functions. Although these methods have previously proven themselves to be useful, the techniques extend far beyond a cell's natural state. As the study of biology progresses, we now understand that a single gene does not necessarily have a single function, but rather is intertwined within a network and participates in multiple functions[21-23]. In addition, gene disruption or over-expression is not applicable to all genes and is an insufficient method for gaining a comprehensive understanding of endogenous functions. A more detailed and precise understanding of a gene in the context of its intricate associations with other genes requires a new method by which genes can be studied more closely to their endogenous levels.

Commonly, promoters with different strengths are used to study the effects of protein abundance. Many stronger promoters such as pGAL1, pTEF2 and pADH1 have been characterized and used to fine-tune gene expression in yeast. Proteins with endogenously strong promoters can be easily under-expressed by replacing their native promoters with weaker ones. However, performing under-expression via a promoter change is experimentally more challenging when many of the endogenous genes have a low abundance. For instance, according to a very recent experiment involving fluorescence microscopy, the quantified in vivo abundances of yeast mating pathway proteins ranged from 60 to 251 molecules per cell[24]. At such low initial protein abundances, it would be difficult to find a weaker promoter that would allow studies of the effects of under-expression. Another widely used method, RNA interference (RNAi), has many advantages when used in gene knockdown experiments. However, the shortcomings of RNAi include variability in gene repression, incomplete knockdown and nonspecificity of reagents, all of which could yield uncertain experimental results[25-27].

The use of programmed −1RFS to reduce protein abundance is unique

because it can be used to target almost any gene with an adjustable under-expression rate and without challenges such as incompleteness or nonspecific activity. Programmed −1RFS is a widely used translational mechanism, primarily found in viruses, that facilitates the expression of two polypeptides from a single mRNA. This mechanism differs from other types of frameshifts in that it is a predetermined alternate translational mechanism for proteins encoded by two overlapping open reading frames. The application of BWYV −1RFS to *S. cerevisiae* comprises a novel method for under-expressing choice of specific target proteins. This study has shown that variable under-expression is possible by using three kinases (MAPKKK Ste11, MAPKK Ste7, MAPK Fus3) and the scaffold protein Ste5 of the mating pathway to reduce their abundance by 11% to 75%, confirming that method could be applied to different proteins.

In some cases, changes in the abundance of only a single protein can have serious biological consequences. For example, reduced gene expression of the period genes involved in a circadian clock model, the fertility related MSY2 gene, and the PPARδ gene in the context of colon cancer were all shown to have deleterious effects[28-30]. When Fus3 was subjected to under-expression, we observed a decrease in the resulting signal output. Previous studies of Fus3 have shown that the deletion of Fus3 causes a defect in cell cycle arrest, while over-expression decreases mating activity[31, 32]. One proposed explanation suggests that when Fus3 is over-expressed, unphosphorylated and catalytically inactive Fus3 could interfere with active Fus3 in transmitting the signal[33]. This decrease in signal transduction in response to reduced abundance is made more interesting by the fact that Fus3 is the only component induced by pheromone stimulation. Specifically, Fus3 abundance increases by at least 3-fold over the level prior to stimulus input[13, 34]. Since Fus3 is capable of increasing its abundance upon activation, one might think that under-expressing would have little effect or even increase the signal transduction output as the lack in initial abundance could be compensated and the inhibition effect could thus be reduced. However, when Fus3 was under-expressed at a level approximately 75% of the wild-type abundance, the signal transduction ability also decreased

compared to the full level of activity. It appears that despite the induction ability of Fus3, the initial endogenous protein expression level is critical to reaching the full capacity for signal transduction. Our results, combined with previous reports, revealed that wild-type Fus3 expression has evolved to yield a maximum signal output.

Furthermore, this experimental technique could be applied to studies of various diseases ranging from neurodegenerative diseases to cancers that arise from over intensified or aberrantly active signal transductions. The current methods of defense are limited to the elimination of the cause or the use of inhibitors[35, 36]. However, in many cases, signal pathways are necessary for differentiation, proliferation, and survival, making elimination or inhibition far from ideal curative approaches. Instead, signal reduction by manipulation within the pathway could be developed into an effective and alternative method of restoring the signaling pathway to a normal state. The under-expression mechanism shown here and the reduction in signal intensity resulting from under-expression warrant further exploration in treatment development

In conclusion, this study describes a new method for inducing protein under-expression in yeast along with direct ways for protein abundance verification and experimental applications. This technique is a novel way of controlling protein expression levels and could become as experimentally useful as deletion and over-expression. It may also be used to study signaling pathway modulation by strategically slowing and reducing processes or preventing signaling activation via component manipulation.

CHAPTER 2. Integrated study of modifying protein abundances and mathematical modeling revealed core characteristics of the Yeast MAP kinase pathway

INTRODUCTION

Signal transduction networks have been field of intensive study for the past three decades. Among from-membrane-to-nucleus signaling pathways, most prokaryotic signal transduction systems and a few eukaryotic pathways operate on just a single protein kinase to deliver the massage. Interestingly, mitogen-activated protein kinase (MAPK) cascade seems to prefer employing three kinases to relay messages, which is generally found in eukaryotes for many different functions[22, 36, 37]. MAPK cascade consists of three protein kinases that are commonly found as a part of a signaling pathway existing in different isoforms for each of the cascade in eukaryotic cells. In a prototypical mating MAPK pathway of S. cerevisiae, Ste11, Ste7 and Fus3 are the three components that transmit signal by sequential activation. Ste11, MAPKKK, activates Ste7, MAPKK[37]. Activated Ste7 activates Fus3, MAPK, functioning as a signal relaying module. It is appealing to think that reasons behind evolving into the three kinase arrangement are for signal amplification[38]. However, without a genetic or biochemical experimental evidence, the concept still remains unsupported. Questions such as how the magnitude, speed, and duration and specificity of the signal through the cascade are orchestrated still remains. The rate-determining step, the neck of a funnel of the three tiered kinase has not been yet determined, which has long been a big question among scholars studying MAP kinase pathways. As the concept of the rate-determining step is important to the optimization and understanding of a process, this finding will be useful for future work on engineered signaling pathways with novel therapeutic or biotechnological functions.

To identify the rate-determining step in the mating MAPK pathway, seven different levels of kinase expression were established for ste11, ste7 and Fus3. Over-expression of the kinases was done by using stronger promoters, CEN/ARS and 2 micron plasmids that carry each kinases, while under-expression of the kinases were made using ribosomal frameshifting pseudoknot of beet western yellow virus (BWYV). Once seven different expression levels of kinases were

established, we could manipulate expressions of the three kinases for identification and analysis of the rate-determining step and other regulation mechanisms of the yeast mating pathway. Initially, the abundances of kinases were modified one at a time to examine how expression level of each kinase effect overall signal transduction output. Then, two kinases were modified at the same time to see if it could cause other changes to the signal output. We also integrated experimental results with mathematical model developed for simulation and prediction to better understand rate-determining step and signal amplification and to utilize the MAP kinase pathway.

MATERIALS AND METHODS

Yeast strains and growth conditions

Studies were done in the *Saccharomyces cerevisiae*. Strains used as hosts for transformation with various kinase expressing vectors were SH153 (*MAT***a**, *trp1, leu2, ura3, his3, mfa::pFus1-LacZ, kss1::NatR, ste11::His3*) for ste11s, SH152 (*MAT***a**, *trp1, leu2, ura3, his3, mfa::pFus1-LacZ, kss1::NatR, Ste7::His3*) for ste7s, RB210 (*MAT***a**, *trp1, leu2, ura3, his3, mfa::pFus1-LacZ, Fus3::KanR, kss1::NatR*) for Fus3s and SH018 (*MAT*a, leu2, trp1, his3, mfa::Fus1-LacZ, Ppq1::HIS5) for ppq1 experiments. RB206 (*MAT***a**, *trp1, leu2, ura3, his3, mfa::pFus1-LacZ, kss1::NatR*) was used as a wildtype strain. The yeast cells were grown at 30℃ in selective mediums for maintaining plasmids. Glucose (2%, w/v) was used as a carbon source. A peptide corresponding to the mating pheromone, α-factor, was chemically synthesized using fluorenylmethoxycarbonyl (F-moc) chemistry and was purified by high-performance liquid chromatography (HPLC). Gene knockouts and substitutions were conducted using standard gene disruption or substitution techniques.

Template construction for over-expression and under-expression of proteins

Table 2 shows the plasmids that were used in this study. All plasmid constructions were confirmed by sequencing and all yeast genomic integrations and deletions were confirmed by yeast colony PCR. Constructs for over-expression were made by use of CEN/ARS vector, 2-micron vector and replacing promoters with stronger strength, such as pADH1 and pTEF2. Under-expression of proteins was achieved through programmed -1RFS described in part1.

Cell preparation and fluorescence-activated cell sorting (FACS)

Cells grown in overnight culture were diluted to an OD_{600} of 0.2 in a selected

medium with 2% dextrose (w/v) as a carbon source and grown to mid-log phase (OD_{600} = 0.5). For FACS analysis of pFus1-EGFP expression, 300 μl of individual cell cultures were transferred to 5-ml tubes and sonicated for 3 s to separate cell clumps. Subsequently, 10,000 cells per sample were analyzed using a flow cytometer (FACSCanto; BD Biosciences, San Jose, CA, USA). Cells were treated with α-factor at a final concentration of 1 μM for up to 2 h to trigger the mating signal. Time point 0 denotes pre-stimulation time point and 30, 60, 90, and 120 min represent the time intervals after stimulation. All transfected cell populations were 100% viable based on forward and side-scatter parameters. Three independent experiments were performed in triplicates.

Cell Lysis, Immunoprecipitation and Immunoblotting

Cell cultures were grown to mid-log phase (OD600=0.7) in a selective medium containing glucose (2%, w/v) before harvesting. For triggering of the mating pheromone pathway, cell cultures were treated with α-factor at a final concentration of 1~10μM. The cells were lysed using glass beads in Y-PER lysis solution (Pierce) containing protease and phosphatase inhibitor cocktails (Sigma-Aldrich). The concentration of total protein in the lysate was measured using a Bradford Assay kit (Bio-Rad). In order to purify the HA-tagged Ste7 variants proteins from the lysate, the cleared lysate was mixed with anti-HA affinity gel (A2220; Sigma), and then incubated at 4℃ for 4 hrs with gentle rocking. The beads were washed four times with ice-cold TST buffer (50 mM Tris-Cl, pH 7.5, 150 mM NaCl, 0.1% NP-40). The washed beads were resuspended in SDS sample buffer and were separated by 10% SDS-PAGE (sodium dodecyl sulfatepolyacrylamide) gel electrophoresis. Proteins separated by SDS-PAGE were transferred to nitrocellulose membranes (Whatman). The membranes were blocked with 5% skim milk in TBST (1% Tween 20) for 1 h at room temperature and were then incubated with the appropriate primary antibodies for overnight at 4℃. The antibodies used were as follows: anti-Fus3 (yN-19; Santa Cruz Biotechnology),anti-phospho-p44/42 (9101S; Cell

Signaling Technology),anti-Myc (F1804, Sigma-Aldrich), anti-HA (sc-805; Santa Cruz Biotechnology), anti-phosphoSerine (05-1000, Millipore), anti-phosphothreonine (05-1000, Millipore), anti-phosphotyrosine (05-1000, Millipore), anti-GST (27-4577-01, GE healthcare), and anti-polyhistidine (H1029, Sigma-Aldrich)antibodies. The membranes were washed several times with TBST and incubated with horseradish peroxidase-conjugated anti-rabbit (Cell Signaling Technology), anti-goat (Santa Cruz Biotechnology), or anti-mouse (Sigma-Aldrich) secondary antibodies. Proteins were detected with an LAS-3000 (Fuji) imaging system using the West Pico Chemiluminescent Substrate (Pierce) according to the manufacturer's instructions. For LC-MS/MS analysis, the proteins were separated by 10% SDS-PAGE and stained using Coomassie Brilliant Blue (CBB) R250 dye.

Mathematical model

In order to study which underlying cellular mechanisms can potentially underlie the dynamic responses of signal transduction pathway, we developed a mathematical model that combines interaction network of essential kinases (*Ste11*, *Ste7* and *Fus3*) and gene expression (*Fus1*) in yeast mating pathway. We considered all possible network topologies from three essential proteins. Similar approach is found from (Ma et al., 2009). Each link of the network can have one of three functions: activation, inhibition, and zero interaction. We assumed that two activation linkages exists (Ste11 → Ste7 and Ste11 → Ste7 → Fus3), thereby the number of possible network topologies is $3^7 = 2187$.

We used ordinary differential equations to describe interactions of kinases (*Ste11*, *Ste7* and *Fus3*). We assumed that each node has active (e.g., *Ste11*) and inactive state (e.g., $Ste11_T - Ste11$), and total amount is conserved to have constant concentration value (e.g., $Ste11_T$). Activation means that inactive state of a node is converted to active state. For example, active state of *Ste11* would convert inactive state of *Ste7* into active state by the rate $v = kSte11(1 - Ste7)/[(1 - Ste7) + K]$. Inhibition means that active state of a node is converted to inactive state. If a node,

for example, A inhibits *Ste7*, then active state of A would convert active state of *Ste7* into inactive state by the rate $v = kASte7/[Ste7 + K]$.

As each converting processes can be assumed as enzymatic reactions, we used Michaelis-Menten equation for reaction velocities. Rate equations for the three kinases are modeled as follows:

$$\frac{dSte11}{dt} = \sum_{\mathrm{i}} k_{X_i Ste11} X_i \frac{(Ste11_T - Ste11)}{(Ste11_T - Ste11) + K_{X_i Ste11}} - \sum_{\mathrm{i}} k'_{Y_i Ste11} Y_i \frac{Ste11}{Ste11 + K'_{Y_i Ste11}}$$

$$\frac{dSte7}{dt} = \sum_{\mathrm{i}} k_{X_i Ste7} X_i \frac{(Ste7_T - Ste7)}{(Ste7_T - Ste7) + K_{X_i Ste7}} - \sum_{\mathrm{i}} k'_{Y_i Ste7} Y_i \frac{Ste7}{Ste7 + K'_{Y_i Ste7}}$$

$$\frac{dFus3}{dt} = \sum_{\mathrm{i}} k_{X_i Fus3} X_i \frac{(Fus3_T - Fus3)}{(Fus3_T - Fus3) + K_{X_i Fus3}} - \sum_{\mathrm{i}} k'_{Y_i Fus3} Y_i \frac{Fus3}{Fus3 + K'_{Y_i Fus3}}$$

where X_i is activating enzymes that can be *Ste11*, *Ste7*, *Fus3* or basal level activating enzyme and Y_i is inhibiting enzymes that can be *Ste11*, *Ste7*, *Fus3* or basal level inhibiting enzyme. The basal level enzymes for activation and inhibition are assumed to have nonzero functionality.

We assume that the expression rate of reporter gene (Fus1-GFP) can be modeled by the sum of a basal production rate, basal degradation rate, and a Hill function. Independent variable of the Hill function is active form of *Fus3* (*Fus3pp*). Then, the expression rate of *Fus1* is modeled as follows:

$$\frac{dFus1}{dt} = \frac{A_{Fus1}[Fus3_{PP}]^n}{[Fus3_{PP}]^{\mathrm{n}} + K_{Fus3}^n} + k_S - k_D[Fus1]$$

where A_{Fus1}, n, K_{Fus3}, k_S, and k_D are maximal expression rate, Hill coefficient, Michaelis-Menten coefficient, basal expression rate, and degradation rate, respectively. The steady state solution of above equation is given as follows:

$$[Fus1] = \frac{1}{k_D} \frac{A_{Fus1}[Fus3pp]^n}{[Fus3pp]^n + K_{Fus3}^n} + \frac{k_S}{k_D}$$

Published experimental data (Chapman and Asthagiri, 2009), shows that the functional relation between *Fus3* and *Fus1* can be assumed as a linear function in steady state. The linear function can be derived under the conditions $K_{Fus3}^{n} \gg Fus3pp$ and $n = 1$, and modeled as follows:

$$[Fus1] = a[Fus3pp] + b$$

where a and b are $\frac{\mathrm{A}}{\mathrm{k_D} K_{Fus3}}$ and $\frac{\mathrm{k_S}}{\mathrm{k_D}}$, respectively. The parameters of the linear function are estimated as: $\mathrm{a} = 0.4915$ and $\mathrm{b} = 0.623$ ($\mathrm{r}^2 = 0.97$).

In-gel digestion, LC-ESI-MS/MS analysis and identification of peptides and proteins

The immunoprecipitated protein was separated by10% SDS-PAGE followed by staining with Coomassie Brilliant Blue (CBB) R250 dye (Usb). The target size band was sliced, after which we performed in-gel tryptic digestion as previously described[39, 40]. The tryptic peptides produced by the trypsin digestion were analyzed by LTQ-XL mass spectrometry (Thermo Finnigan, San Jose, CA) coupled with an Eksigent-Nano-Ultra-UPLC (Eksigent Technologies, CA). The digested peptides were loaded onto trap column (100μm x 1.5 cm; homemade) packed with C18 regular 5μm sized resin which loaded peptides were eluted with a linear gradient from 3 to 50% solvent B (0.1% formic acid in ACN) for 35 min at a flow rate of 300nL/min. The eluted peptides, separated by the analytical column (75μm x 1 cm; homemade), were sprayed into nano-ESI source with an electrospray voltage of 1.85 kV. The LTQ-XL mass spectrometer was operated in data-dependent mode. A scan cycle was initiated with a full scan of high mass accuracy (m/z 300-2000) followed by MS/MS scans of the five most abundant precursor ions. The normalized collision energy used was 35%. The repeat duration for dynamic exclusion was 30s, repeat count was set to 1, the dynamic exclusion duration was set to 180s, the list of dynamic exclusion was 50, and the exclusion mass width was 1.5 Da.

The acquired MS/MS spectra were generated by Extract_Msn in Bioworks

software (v. 3.3.1) and searched against the NCBI *S. cescerevisiae* RefSeq protein sequence database (date 2011.08.29 / 67067 protein entries) with the SEQUEST in BioworksBrowser (v. 3.3.1) using the following parameters: enzyme = trypsin, precursor tolerance = 1.5 Da, fragment tolerance = 0.8 Da, oxidation on Met (+16 Da), alkyation on Cys (+57 Da), phosphorylation on Ser(+80 Da), number of missed cleavages = 2.

RESULTS

Seven levels of protein expression

To measure the effects of kinase abundance in signal transduction, we constructed seven levels of expression that varied the kinase abundance. The difficulty of under-expressing a protein to a desired level is one of the reasons that made this challenging. We have applied viral programmed -1 RFS described in part1 to under-express kinases of interest. A yeast strain without kss1 was set as the base point, an endogenous level of expression. A kinase sitting on a 2-micron vector was used to express two-level higher abundance and CEN/ARS vector was used to express one-level higher abundance of the endogenous level. A programmed -1 RFS element that is known to only translate 30% in virus was used as two-level down expression construct and in-frame construct of the same sequence was used as one-level down construct as it should theoretically have efficiency to translated kinase about 70% of the time compared to the base level. Firefly luciferase (fluc) gene was attached to the end of each kinase on each construct to verify how much of the kinase is actually expressed as a protein.

For instance, Fus3 on 2-micron vector expressed about 6 times higher compared to the Fus3 on CEN/ARS vector, which expressed approximately 2 time more than the endogenous (endo) abundance. Stronger promoters such as pTEF2 and pADH1 were used to increase Fus3 abundance even higher, that expressed about 17 and 13 time higher than the endogenous level of expression, respectively. Frameshifted Fus3 expressed about 25% of the endogenous Fus3, while in frame construct (in) expressed about 60%. Fus3 expression levels of seven constructs were also verified again by western blotting with Fus3 antibody (Fig. 5).

Same constructs were applied to kinases Ste11 and Ste7 of the mating pathway. In case of Ste11, the MAPKKK, highest expression level was achieved at 41 times the endogenous abundance whereas lowest under-expression yielded 37%

Figure 5.

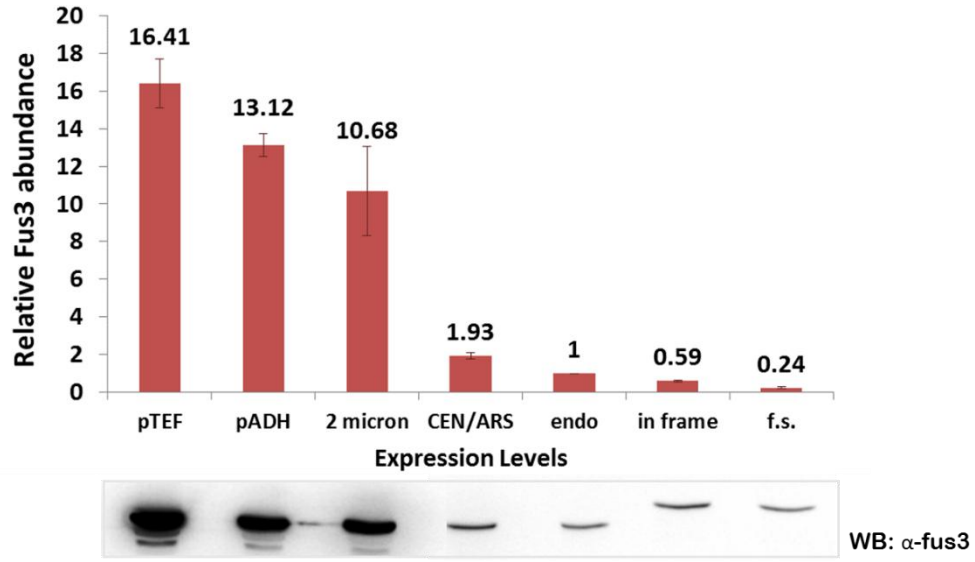
Relative Fus3 abundance
20
18
16
14
12
10
8
6
4
2
0
16.41
13.12
10.68
1.93
1
0.59
0.24
pTEF
pADH
2 micron
CEN/ARS
endo
in frame
f.s.
Expression Levels
WB: α-fus3

Figure 5. Protein abundance range of Fus3.

Fus3, MAPK, was over-expressed with stronger promoters such as pTEF2 and pADH1 or with high copy plasmids such as 2 micron and CEN/ARS. Fus3 was also under-expressed using frameshift elements. Graph shows values obtained from luciferase assay with fluc tagged Fus3 constructs. Same proteins were detected with Fus3 antibody for a visual confirmation of protein abundances. Representative results of multiple trials (n = 3) are shown.

(Fig. 6a). Ste7, the MAPKK, resulted in expression ranging from about 63 times higher to expressing only 60% compared to the endogenous Ste7 abundance (Fig. 6b). The differences in expression levels comes from the fact that endogenous abundances of these kinases are different to begin with. It is well known that Fus3 is the most abundant kinase of the three, but according to previous reports, depending on the methods of detection used, the abundances differ from experiment to experiment, in some cases substantially. Here, we measured endogenous abundance of Ste11, Ste7 and Fus3 by luciferase assay with expression of fluc attached to the ends of each kinase. Ste11 had the lowest expression level and setting that as the standard, Ste7 and Fus3 existed about 1.3 times and 6 times higher, respectively (Fig. 6c). Taking that into account, expression of all the constructs ranged in three folds in logarithmic scale (Fig. 6d).

Single perturbation showed Ste11 to be the rate-determining component.

Single perturbation where the protein abundance of kinases was changed one at a time was performed to observe their contribution to the overall outcome of the signal response. Ste11, MAPKKK, showed biggest influence over the signal output. Decrease in the Ste11 abundance yielded decrease in response outcome, which would imply that abundance of Ste11 is important to the transduction of signal through the pathway. Also, increase in Ste11 abundance increased response outcome exceeding the output level of the endogenous output by about 2.5 times (Fig. 7a). The output response changed somewhat proportionally to the abundance change of Ste11. Therefore, Ste11 seems to be the rate-determining component of the mating pathway. It seems that endogenous Ste11 exists in an abundance that does not maximize the output, but at a midpoint where it has a potential to increase the response outcome.

On the contrary, perturbation of Ste7 and Fus3 abundance had little or no effect on the signal outcome. Even with abundance change ranging in three folds,

Figure 6.

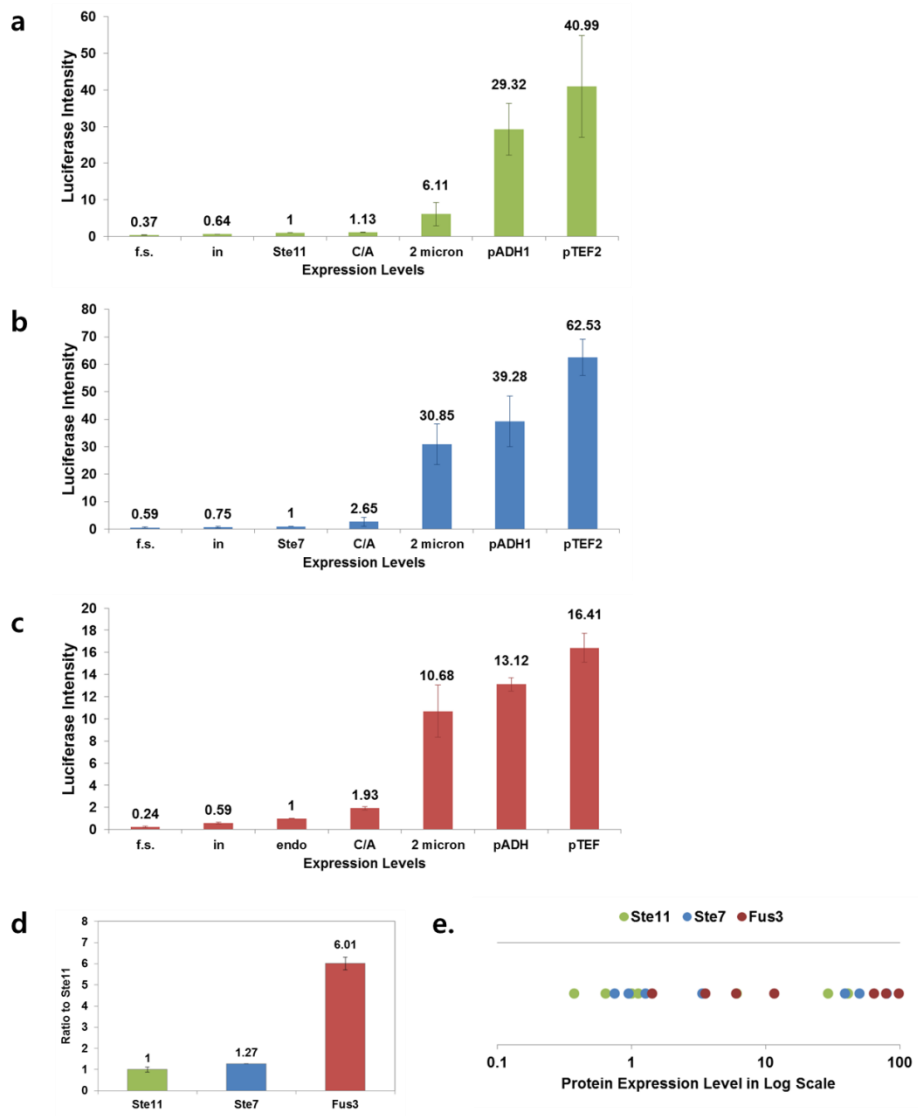
a
Luciferase Intensity
60
50
40
30
20
10
0
0.37
0.64
1
1.13
6.11
29.32
40.99
f.s.
in
Ste11
C/A
2 micron
pADH1
pTEF2
Expression Levels
b
Luciferase Intensity
80
70
60
50
40
30
20
10
0
0.59
0.75
1
2.65
30.85
39.28
62.53
f.s.
in
Ste7
C/A
2 micron
pADH1
pTEF2
Expression Levels
c
Luciferase Intensity
20
18
16
14
12
10
8
6
4
2
0
0.24
0.59
1
1.93
10.68
13.12
16.41
f.s.
in
endo
C/A
2 micron
pADH
pTEF
Expression Levels
d
Ratio to Ste11
8
7
6
5
4
3
2
1
0
1
1.27
6.01
Ste11
Ste7
Fus3
e.
Ste11
Ste7
Fus3
0.1
1
10
100
Protein Expression Level in Log Scale

Figure 6. Protein expression of three kinases

(a) Ste11, MAPKKK, was under-expressed at two levels and over-expressed at four levels. Detections were made by luciferase assay. (b) Ste7, MAPKK, was under-expressed at two levels and over-expressed at four levels. Detections were made by luciferase assay. (c) Fus3, MAPK, was under-expressed at two levels and over-expressed at four levels. Detections were made by luciferase assay. (d) Comparison of endogenous abundance of Ste11, Ste7 and Fus3 detected by luciferase assay. Ste11 had the lowest abundance whereas fus3 had highest abundance in absence of stimulation. (e) Comparison of all the constructs from under-expressed to over-expressed of Ste11, Ste7 and Fus3 drawn in one line for a better comparison. Values in the graph represent the means and standard deviations from three separate experiments.

Figure 7.

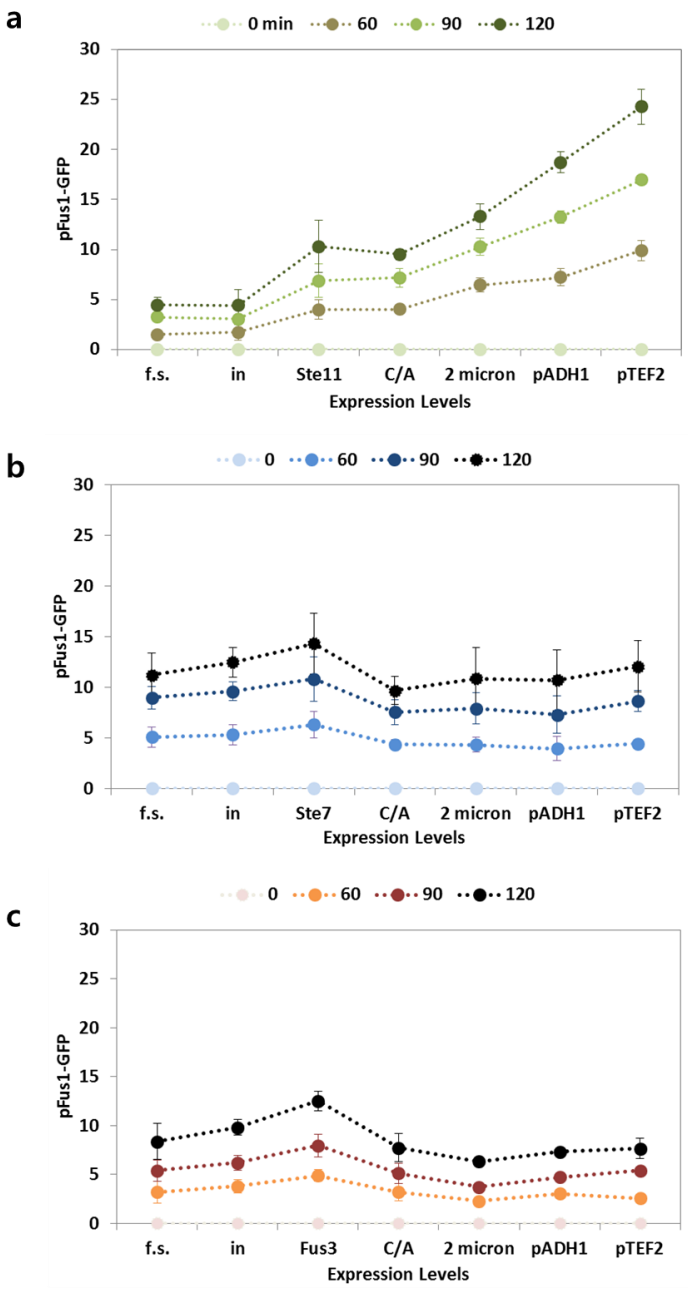
a
0 min
60
90
120
pFus1-GFP
30
25
20
15
10
5
0
f.s.
in
Ste11
C/A
2 micron
pADH1
pTEF2
Expression Levels
b
0
60
90
120
pFus1-GFP
f.s.
in
Ste7
C/A
2 micron
pADH1
pTEF2
Expression Levels
c
0
60
90
120
pFus1-GFP
f.s.
in
Fus3
C/A
2 micron
pADH1
pTEF2
Expression Levels

Figure 7. Single perturbation of kinases.

(a) Under-expressed and over-expressed Ste11 constructs were expressed on a ΔSte11 yeast strain. (b) Under-expressed and over-expressed Ste7 was expressed on a ΔSte7 yeast strain. (c) Under-expressed and over-expressed Fus3 was expressed on a ΔFus3 yeast strain. In all three experiments signal output was detected by GFP expression dependent on the induction of mating induced gene, *Fus1*. Values in the graph represent the means and standard deviations from three separate experiments.

results from MAPKK and MAPK abundance change did not show much difference in the overall response output (Fig. 7b and c). This is a display of a remarkable robustness against perturbation of Ste7 and Fus3, suggesting that some kind of negative regulation is at play between Ste7 and Fus3 to keep the output level steady against perturbation in Ste7 and Fus3 abundance.

Such phenomenon is made more intriguing by the difference in endogenous abundance of three kinases. Ste11 is previously known and observed here as a kinase with lowest abundance. In case of Fus3, it is the most abundant kinase of the three and at the same time its abundance is induced upon pheromone stimulation to the level of about three times higher. Considering these factors, signal flow seems to be amplified between Ste11 and Ste7, while signal is tightly regulated from Ste7 to the induction of mating related genes.

Double perturbation showed synergetic increase between Ste11 and Fus3 and hindrance between Ste11 and Ste7 in signal output.

Since Ste11 showed greatest influence over signal output, we wondered how double perturbation of kinases would affect the output. Change in abundance of Ste11 and Fus3 resulted in a predictable manner as one might have expected from the single perturbation results. Decrease in abundances of both kinases resulted decrease in signal output and increase in abundances of both kinases resulted in increase in signal output (Fig. 8a). Although single perturbation of Fus3 did not affect the outcome, when Fus3 abundance was changed along with abundance of Ste11 the effect was greater than when Ste11 was singly over-expressed. Fus3 and Ste11 showed synergic increase in the output by 4-fold increase in output when both kinases were expressed to the maximum abundance.

Interestingly, double perturbation of Ste11 and Ste7 displayed unexpected hindrance in signal output. While increase in Ste7 abundance alone did not have negative effect on the signal outcome, increase in Ste7 abundance when Ste11

Figure 8.

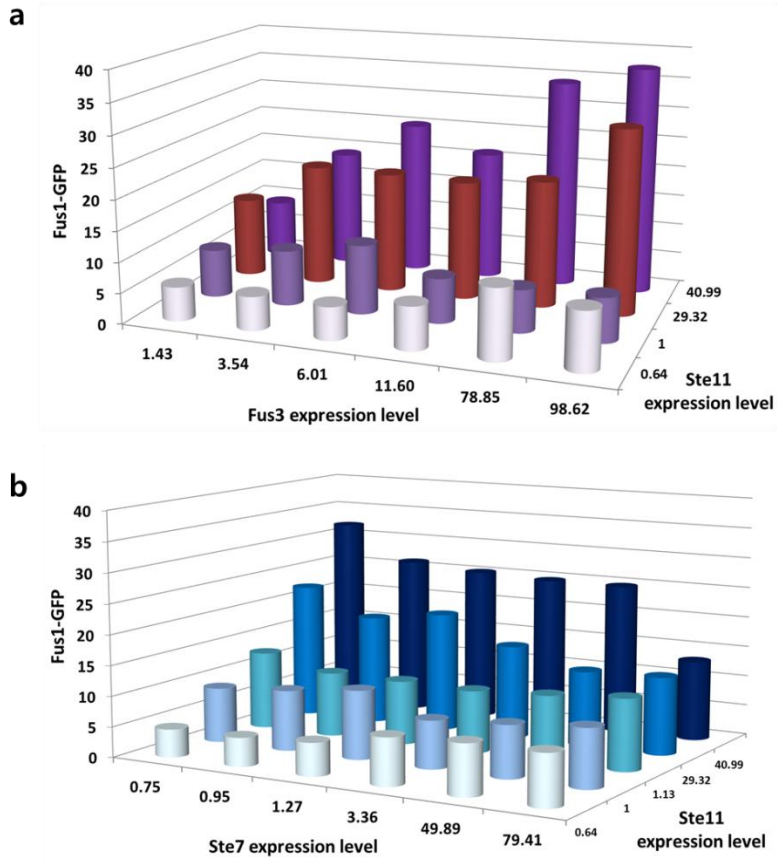
a
Fus1-GFP
40
35
30
25
20
15
10
5
0
1.43
3.54
6.01
11.60
78.85
98.62
Fus3 expression level
40.99
29.32
1
0.64
Ste11
expression level
b
Fus1-GFP
40
35
30
25
20
15
10
5
0
0.75
0.95
1.27
3.36
49.89
79.41
Ste7 expression level
40.99
29.32
1.13
1
0.64
Ste11
expression level

Figure 8. Double perturbation of kinases.

(a) Under-expressed and over-expressed Ste11 and Fus3 constructs were expressed in various combinations on a ΔSte11, Fus3 yeast strain. Signal output was detected by GFP expression dependent on the induction of mating induced gene, *Fus1*. Experimental data were normalized relative to the result of endogenous Ste11 and Fus3 data for representation on a single graph. (b) Under-expressed and over-expressed Ste11 and Ste7 constructs were expressed in various combinations on a ΔSte11, Ste7 yeast strain. Signal output was detected by GFP expression dependent on the induction of mating induced gene, *Fus1*. Experimental data were normalized relative to the result of endogenous Ste11 and Ste7 data for representation on a single graph.

abundance is high had negative effect. Double increase in abundances of Ste11 and Ste7 decreased signal output. To make things more interesting, increase in Ste11 abundance and decrease in Ste7 abundance increased signal output even more than when Ste11 abundance was increased on an endogenous Ste7 (Fig. 8b). Taken together, Ste7 seems to be involved in a negative regulation of the signal output. Therefore, decrease in Ste7 could expand signal pathway potential to increase the output.

Mathematical Modelling revealed a core structure consisting of two negative feedbacks and a positive feedback.

While it is clear that MAPKKK plays the rate-determining role and signal pathway is designed to be robust to perturbations of MAPKK and MAPK, how this is managed remains unclear. To gain better insights into the conditions under the MAP kinase pathway is regulated, we created a mathematical model to explore the rate-determining step and the controlling mechanism of the yeast decision making system. We constructed a three component model with all possible connections or nodes, which comes to total of 2187 structures (Fig. 9a). Three component stands for Ste11, Ste7 and Fus3 with connections between them that can either be positive or negative. All 2187 structures were analyzed and their likeness to the experimental data was measured to obtain the fitness values (Fig. 9b). Structures according to fitness value can be divided into region 1 and region 2. Differences between structures in region 1 and region 2 are correspondence and deviation. Structures in region 1 were all closely similar to the experimental data and the structural integrity was high showing low variation on multiple simulations. On the contrary, structures in region 2 deviated from the experimental data and the structures showed greater variations on simulations.

Next, we performed synergy analysis to find if existence of certain nodes works together to better fit the experimental data. It turns out presence of some

Figure 9.

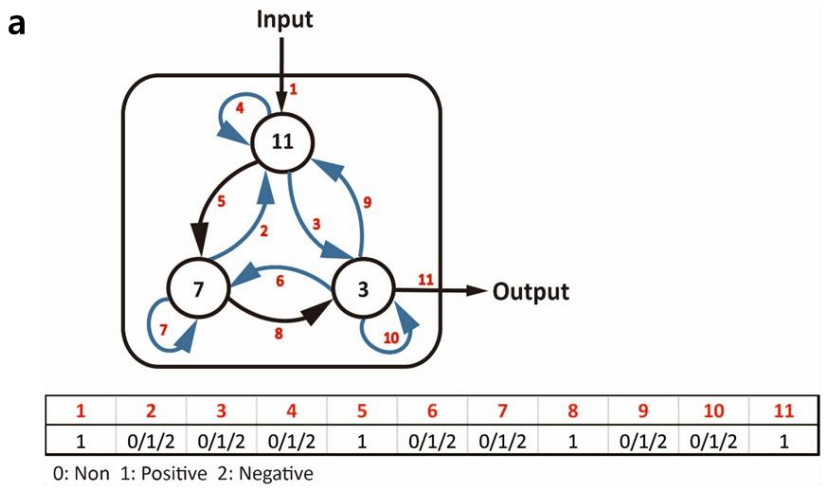

1	2	3	4	5	6	7	8	9	10	11
1	0/1/2	0/1/2	0/1/2	1	0/1/2	0/1/2	1	0/1/2	0/1/2	1

0: Non 1: Positive 2: Negative

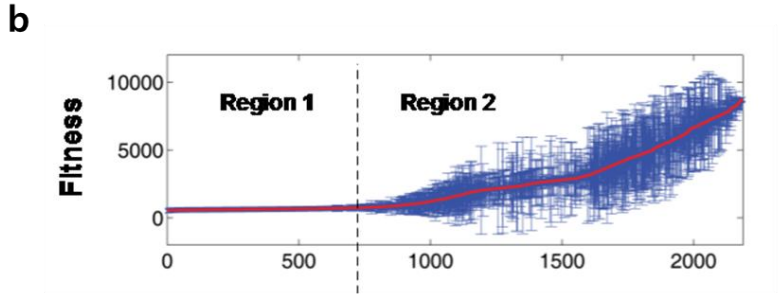

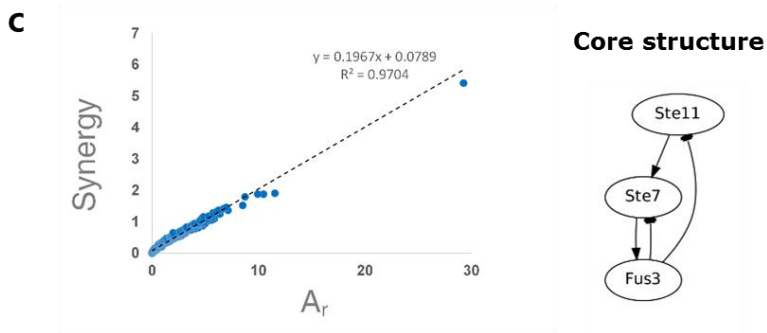

Figure 9. Mathematical modeling and analyses.

(a) Three component model was built to include all possible connection (nodes) between the input and output. 0 represent non-existence of the connection, 1 represents a positive effect and 2 represents a negative effect. Since we know that input, output and activation of upstream component to the downstream component are always present, those were assign 1. (b) Fitness analysis was done by comparing all the structures to the experimental data. Once simulation data were gathered, all structures were subjected to a lineup of ranking from the fittest to the inadequate. (c) Synergy analysis was performed to find if coexistence of certain nodes increase the fitness. The analysis revealed one core structure that distinctively had high synergy value. The core structure found here would be the foundation of the optimal structure.

nodes decrease fitness whereas coexistence of some nodes synergistically increases fitness to experimental data (Fig. 9c). Particularly, a structure with negative feedbacks stemming from MAPK Fus3 to Ste11 and Ste7 singularly stood out. It seems that a majority of model constructs with high fitness consists of these two negative feedbacks as a core structure.

Models were then put through elimination process of getting rid of constructs that doesn't make sense for various reasons (Fig. 10a). For example, in the MAP kinase pathway, the existence of three-tier is essential and the pathway cannot function in the absence of any one of the kinases. Therefore, any structures that are designed to skip a kinase can be eliminated. Also, the response output of a signaling pathway is does dependent. If a construct, upon simulation does not put out a result that shows increase in signal output as stimulation increases those could also be discarded (Fig. 10b). Once we had group of structures that seemed suitable, they were subjected to another round of simulation to be compared to the double perturbation experimental data. As double perturbation experiment yielded unique phenomenon, only few structures fit the profile.

Combined analyses of 2187 structures revealed a single structure that best fitted all aspects of the data. The three component optimal structure had two negative feedbacks stemming from MAPK Fus3 to Ste11 and Ste7 and a positive feedback stemming from MAPKK Ste7 to MAPKKK Ste11 (Fig. 10c).

Ste7 in negatively regulated by negative feedback loop via Ppq1.

Some of the feedback regulations could be explained from previous research. Although we cannot directly prove if activated Ste7 in turn activate more Ste11, it is well known from experiments that constitutively active Ste11 increases the signal response outcome, while constitutively active Ste7 doesn't. Also, pheromone signal dependent ubiquitination occurs in Ste11 and Ste7, degrading their active forms, which could be working as a negative feedback loop.

Figure 10.

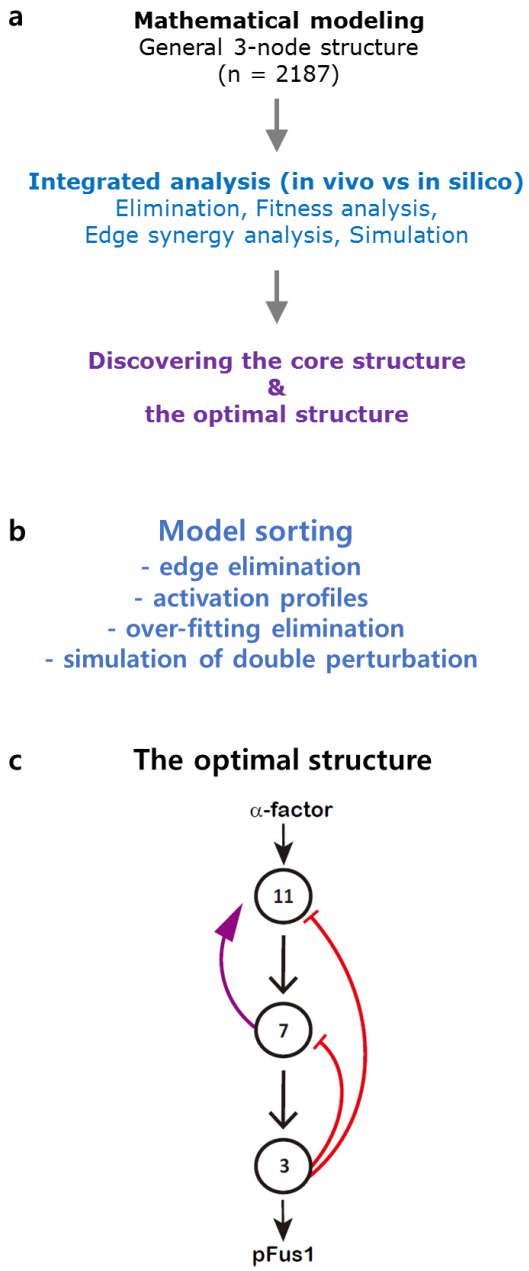
a
Mathematical modeling
General 3-node structure
(n = 2187)
Integrated analysis (in vivo vs in silico)
Elimination, Fitness analysis,
Edge synergy analysis, Simulation
Discovering the core structure
&
the optimal structure
b
Model sorting
- edge elimination
- activation profiles
- over-fitting elimination
- simulation of double perturbation
c
The optimal structure
α-factor
11
7
3
pFus1

Figure 10. Mathematical modeling and analyses.

(a) Process of modeling analyses. After constructing mathematical models, integrated analyses of fitness analysis, synergy analysis, elimination and simulation were performed. These analyses produced the core structure and the optimal structure that could best explain the experimental data. (b) Sorting of model constructs included edge elimination of getting rid of models with unnecessary connections, activation profile analysis of simulating activation profiles to determine functionality of the model, over-fitting elimination by sorting out structure that does not give out a robust outcome, and fitness analysis with simulation of double perturbation. (c) The result of integrated analyses produced a single well-fitting optimal structure with one positive feedback and two negative feedbacks.

Additionally, we identified a novel negative feedback loop via a relatively unknown phosphatase Ppq1[41]. When Ppq1 is overexpressed, signal outcome measured by mating efficiency decreases. On the contrary, mating efficiency increases if Ppq1 is deleted. To identify Ppq1 as a negative regulator, we investigated whether the phosphorylation level of mating pathway related kinases change by Ppq1. For immunoprecipitation, HA-tagged Ste7 was overexpressed from the GAL1 promoter and obtained using anti-HA affinity gel. Ste7 has some degrees of phosphorylation modifications in the absence of pheromone and the modification increases upon mating signaling by pheromone stimulation. In comparison of Ste7 phosphorylation level with Ppq1 deletion strain, remarkable decrease in Ste7 phosphorylation at serine and threonine was observed when Ppq1 was overexpressed (Fig. 11a). On the contrary, Ste11 phosphorylation level did not depend on Ppq1 (Fig. 11b). In the case of Fus3, only tyrosine site seems to be dependent on the existence of Ppq1 as the phosphotyrosine level increase when Ppq1 is deleted (Fig. 11c).

Next, using LC-MS/MS analysis, we identified phosphorylation site in Ppq1 that regulates the catalytic activity of Ppq1 (Fig. 12a). The Ser208 in Ppq1 corresponds to the phosphorylatable serine residue within the consensus sequence Pro-X-Ser-Pro, which is likely to be phosphorylated by MAPK. Observing the induction level of mating related gene, Fus1, we found that the S208E, phosphomimic mutant of Ser208 in Ppq1, exhibited stronger inhibition than wild-type Ppq1 (Fig. 12b and c). Combined data show that Ppq1 down regulates mating signaling through dephosphorylation at several sites in Ste7. During adaptation to stimulation, Ppq1 is phosphorylated at conserved Ser208, perhaps by Fus3.

From integration of experiments and mathematical modeling, we propose a fundamental structure and regulation of the yeast mating MAP kinase pathway (Fig. 13). It consists of three components that delivers the signal managed by a positive feedback for signal amplification and two negative feedbacks that restrict the further changes to the signal for a stable output, yielding a decisive outcome.

Figure 11.

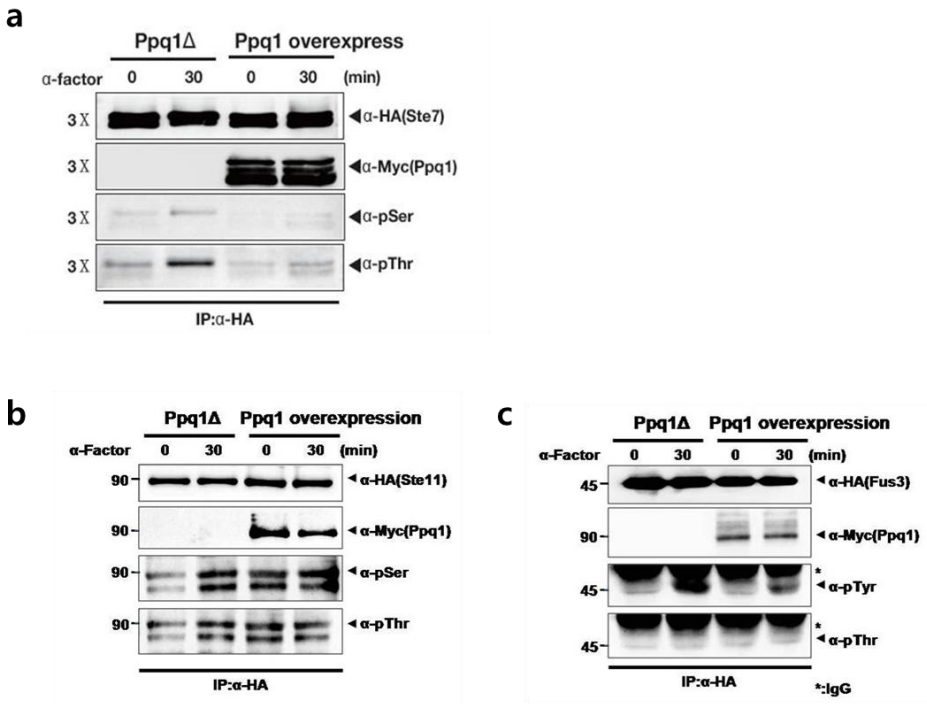
a
Ppq1Δ
Ppq1 overexpress
α-factor 0 30 0 30 (min)
3X
α-HA(Ste7)
α-Myc(Ppq1)
α-pSer
α-pThr
IP:α-HA
b
Ppq1Δ
Ppq1 overexpression
α-Factor 0 30 0 30 (min)
90
α-HA(Ste11)
α-Myc(Ppq1)
α-pSer
α-pThr
IP:α-HA
c
Ppq1Δ
Ppq1 overexpression
α-Factor 0 30 0 30 (min)
45
90
α-HA(Fus3)
α-Myc(Ppq1)
α-pTyr
α-pThr
IP:α-HA
*:IgG

Figure 11. Ppq1 recognizes and dephosphorylates Ste7.

(a) Ppq1 dephosphorylates Ste7 in vivo. HA-tagged Ste7 was expressed with or without myc-tagged Ppq1 in Ppq1Δ (SH018) cells and were exposed to 10 μM α-factor for 30 min. HA-tagged proteins were immunoprecipitated using anti-HA affinity gel and then separated by SDS-PAGE. Threonine-phosphorylated (pThr), serine-phosphorylated (pSer), and total proteins were visualized using anti-phosphothreonine antibody, anti-phosphoserine antibody, and anti-HA antibody, respectively. Immunoblot analyses reveal that significant decrease of phosphorylated Ste7 in serine and threonine by Ppq1 overexression before and after pheromone stimulation. (b) Effects of Ppq1 on Ste11. Ppq1 does not seem to affect Ste11 phosphorylation level. (c) Effects of Ppq1 on Fus3. Decrease of Fus3 tyrosine phosphorylation level could result in reduced mating flux by Ppq1.

This figure appeared in: Shim, EY. (2014). *Identification and functional analysis of phosphoprotein in yeast MAPK signaling pathway* (Doctoral dissertation). Seoul National University, Seoul, Korea.

Figure 12.

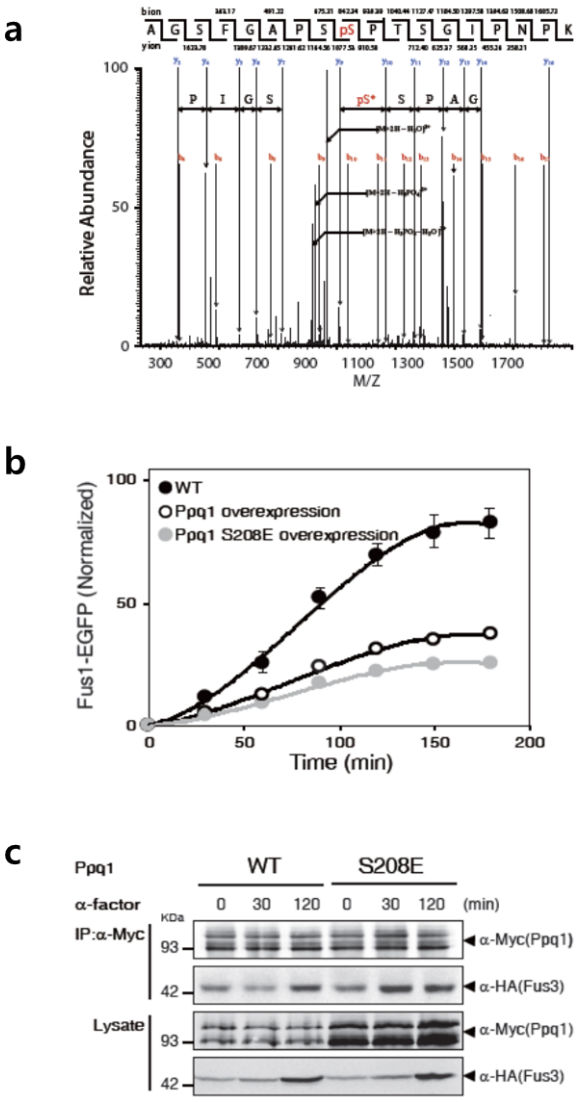
a
b
c
Relative Abundance
M/Z
Fus1-EGFP (Normalized)
Time (min)
WT
Ppq1 overexpression
Ppq1 S208E overexpression
Ppq1
α-factor
IP:α-Myc
Lysate
α-Myc(Ppq1)
α-HA(Fus3)
KDa
(min)

Figure 12. Ppq1 is regulated through Ser208.

(a) Identification of phosphorylation in Ppq1 at conserved Ser208. The Ppq1Δ cells (SH018) bearing myc-tagged Ppq1 were stimulated with 10 μM α-factor for 1 hr. The Ppq1-myc proteins were immunoprecipitated and separated by SDS-PAGE, then subsequently stained with CBB R250. The samples were analyzed by LC-MS/MS. (b) Phosphomimic mutant Ppq1(S208E) represses Fus1 activation stronger than wild-type did. (c) Extracts from Ppq1Δ cells (SH018) harboring Myc-tagged Ppq1 or Ppq1 S208E was subjected to immunoprecipitatio and immunoblotting result shows that the phosphomimic substitution mutations S208E causes increase of binding affinity with Fus3, suggesting that the increase of mating repression by phosphorylation at Ser208 might be caused by effective recruitment of Ppq1 to the substrate.

This figure appeared in: Shim, EY. (2014). *Identification and functional analysis of phosphoprotein in yeast MAPK signaling pathway* (Doctoral dissertation). Seoul National University, Seoul, Korea.

Figure 13.

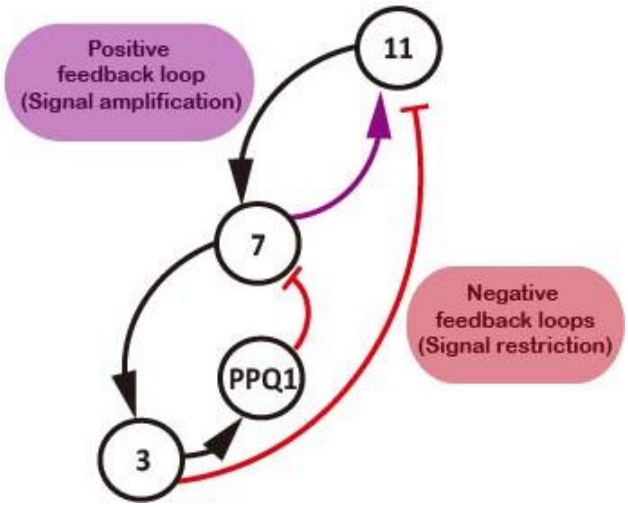
Positive
feedback loop
(Signal amplification)
11
7
PPQ1
3
Negative
feedback loops
(Signal restriction)

Figure 13. The optimal structure and regulations.

The optimal structure consists of positive feedback loop for signal amplification and negative feedback loops for signal restriction, one in particular via Ppq1.

DISCUSSION

Signal transduction pathways are essential for the survival of cells and a useful method of controlling the input stimulus and output results. It is at the center of responding to environmental cues[42-44]. Therefore, signal pathways are frequently used in synthetic biology to engineer pathways to produce the target product[45-47]. There is a strong connection between signaling research and disciplines of synthetic biology. Therefore, elucidating the fundamentals of the existing biological signaling pathways such as the rate-determining step, signal amplification, and positive or negative regulations are important. It is now well known that signal pathways are made up of a complex network, therefore, it is easy to get lost in it. At a time like this, it is important to identify the minimal requirements to better understand the mechanisms for diagnosing and treating various signaling related diseases and for programming cells to do desired functions.

Since observing exactly how much of a signal is transferred from input to the output though MAP kinase pathway is nearly impossible, due to its size and minimal presence in the cellular pool, we developed an alternative method to determine the rate-determining component among the three component system. By decreasing and increasing the abundance of each kinase, we could restrict or expand the pathway capacity to give flexibility to the pathway. The results showed that only MAPKKK Ste11 had influence over the control of pathway capacity, while the signal output was robust to the changes in Ste7 or Fus3.

To better explore the minimal requirements of the efficient signal transduction, we created a mathematical model of simplest form, but with all the possibilities. The three component model with various possible connections were made, simulated and compared with the experimental results. Multiple analyses in diverse aspects produced a core structure and an optimal structure that could best explain the phenomenon. The structure essentially has a two negative feedbacks stemming from MAPK Fus3. Existence of these two would be why the signal output was so robust to the changes in Ste7 and Fus3. Additionally, a newly found

positive feedback stemming from Ste7 to Ste11 would explain the increase in pathway capacity as abundance of Ste11 increased. We have manipulated to increase the presence of Ste11 from the beginning, but a cell had its own way of amplifying the signal with a positive feedback loop.

Next, we further explored the negative feedback working at Ste7. Ppq1 is a pheromone dependent down regulator of the yeast mating pathway. It interacts with Ste7 in vivo and mainly works to dephosphorylate active Ste7. The conserved phosphorylated site in Ppq1, Ser208, is only found upon pheromone stimulation and likely phosphorylated by Fus3.

In theory, it is an ideal design for controlling the process of from input to output. In the very beginning, amplification would occur between Ste11 and Ste7 by the positive feedback. But once it reaches downstream, flexibility of the signal is reduced as the negative feedbacks restrict the signal. Since MAP kinase pathways are cell's way of making a decision, it is preferable to contemplate early on and then sticking to a decision for fast and sharp response. The minimal signaling modules discovered here through experimental and systematic integrated analyses will provide mechanistic detail to the future of creating biotechnologically and biomedically useful synthetic cellular devices.

CHAPTER 3. MAPK pathway-originated and inherent stochasticity in signal responses contribute to diversity while preserving consistency

INTRODUCTION

Diversity is established at multiple ecological levels from an individual to the ecosystem to ensure survival and natural sustainability for all life forms[48-50]. Organisms of every class exhibit multiple layers of diversity, ranging from ecosystem to genetic diversity, to reduce the incidence of unfavorable inherited traits and to increase survival chance. Genetic diversity, introduced through mutation and sexual recombination, is crucial for the adaptation and survival of organisms existing in temporally and spatially variable environments[51, 52]. Intriguingly, diversity exists even among microorganisms from prokaryotes to eukaryotes[53-58]. The first experimental observation from a cell population was reported in the 1950s showing variation in beta-galactosidase production[59].

With advances in single-cell technology, researchers began studying the mechanisms and consequences of noise in cells[60, 61]. Previous studies have shown that genetically identical cells exposed to the same environmental conditions exhibit variation in molecular contents[62-65]. Some studies experimentally demonstrated that noise primarily arise from differences in the regulation of gene expression, leading to stochastic fluctuations in their abundance and activities[66-68]. Furthermore, a single-cell level study showed that such variations in system output are relatively constant over time, suggesting that such variation arise from preexisting cell-to-cell difference regardless of stimulation[69]. Another study investigated changes in signal response noise over few time points, and found an initial increase in the noise level after pheromone stimulation, followed by decrease to the basal noise level[64]. The consequences of such variations can be viewed as either unavoidable side effects or a chance that could potentially be beneficial. Few studies on the metabolic networks of *Escherichia coli* and yeast have demonstrated competitive advantage in fluctuating environments with observation that fluctuations in gene expression influence the transition between the on-and-off states[70-72]. Although previous studies have made interesting discoveries, they analyzed dispersion at certain time points, examining variations relative to mean values.

Yeast has long been the popular and classical eukaryotic model for biochemical research as well as in studies of evolution and behavioral science[73-75]. The mating pathway, one of the most studied MAPK pathways, is a decision-making system with the potential to cause big losses if fusion with the opposite haploid fails. A recent study on the cost of sexual signaling found that the handicap principle holds true, meaning that a stronger mating signal indicates a superior genetic quantity[76]. If variations in response to pheromones among different yeasts can be explained by genetic fitness, how do we explain variations observed within an isogenic population of yeast?

Here we studied cell-to-cell variations of signal response profiles (SRPs) derived from the yeast mating pathway. In *Saccharomyces cerevisiae*, the pheromone induces mating-related genes that typically exhibit a profile with a rapid increase after stimulation up to a peak, followed by a return to the basal level[34, 41, 77]. Using the yeast-on-a-chip (YOC) system, we were able to time-track single cells and obtain reporter gene expression profiles, thus yielding SRPs. We examined stochasticity by comparing SRPs to determine the response profile stochasticity (RPS), which uncovered new aspects of diversity. The analysis revealed a high level of RPS, which originated from signal transduction through the MAPK pathway and displayed distinction in response time and duration. To characterize these observations, we evaluated RPS in same cells repeatedly exposed to pheromone stimuli and also compared RPS values of mother and daughter cells. Intriguingly, we did not identify any correlations of RPS values in either case, suggesting that RPS is a non-genetic and inherent trait.

MATERIALS AND METHODS

Strains and plasmids

The *S. cerevisiae* strains used in this study were SH129 (SO992 fus1::yEGFP-SpHIS5, gpd1::Tdimer2-CaURA3), SH130 (SO992 fus1::yEGFP-SpHIS5, stl1::Tdimer2-CaURA3), SH133 (SO992 fus1::yEGFP-CLN2(PEST)-His3MX6, gpd1::Tdimer2-CaURA3), SH177 (SH129 kss1::Trp1), and SH178 (SH129 fus3::Trp1). SH129, SH130, and SH133 were generated via a PCR-based tagging technique, using pKT128, pKT176, and pSH1133 [pFA6a-yEGFP1-CLN2(PEST)-His3MX6], respectively, as template[78]. SH177 and SH178 were generated via PCR-based gene deletion, using pFA6a-GFP(S65T)-TRP1 as a template[15, 16]. SH130 was transformed with the pSH1277 vector (TRP1, ARS/CEN plasmids) which expresses Ste12 from a GAL promoter for overexpression of Ste12. *Ste5*, *Ste11*, *Ste7*, and *Fus3* genes were individually sub-cloned into p416 ADH or p424 GPD vectors. SH129 were transformed with p416 ADH-Ste5, p416 ADH-Ste11, p416 ADH-Ste7, or p416 ADH-Fus3 vector for overexpression of Ste5, Ste11, Ste7, or Fus3, respectively. For higher level of protein expression, SH129 were transformed with p424 GPD-Ste5, p424 GPD-Ste11, p424 GPD-Ste7, or p424 GPD-Fus3 to induce the overexpression of Ste5, Ste11, Ste7, or Fus3, respectively[79]. Yeast cells were grown at 30 °C in YPD medium and selective medium containing 2% (w/v) dextrose as a carbon source. A peptide corresponding to α-factor was chemically synthesized using fluorenylmethoxycarbonyl (F-moc) chemistry and purified by high-performance liquid chromatography. All chemicals and reagents were of the highest grade commercially available. The pKT128, pKT176, pFA6a-GFP(S65T)-TRP1, p416 ADH and p424 GPD vectors were provided by Won-Ki Huh.

YOC

To generate a patterned microfluidic channel, a polydimethyl siloxane (PDMS)

microfluidic mold and polyurethane acrylate (PUA) microwell-patterned slide glass were subjected to plasma cleaning for 45 s (60W, PDC-32G, Harrick Scientific Products Inc., Ossining, NY, USA) and then irreversibly bonded together under slight pressure. The PUA microwells contained hollow cylindrical holes with a diameter and depth of 8 μm[80].

Yeast cell docking

Yeast cell suspension was concentrated to approximately 5.0×10^9 cells/mL via centrifugation for optimal docking efficiency. To assess the cellular response at a single-cell level, a small volume (approximately 0.7 μL) of concentrated cells was introduced into the microfluidic channel by capillary action. After the yeast cells were allowed to settle for a few minutes, the punched hole region was carefully swept using finger-applied pressure. As the meniscus receded over the microwells, single yeast cells spontaneously docked into the microwells. The remaining cells inside the microchannel were washed out using a flow of synthetic complete (SC) medium. Once the floating cells were removed, the microchannel was filled with a fresh SC medium.

Cellular response monitoring

Cellular responses on the YOC system were observed with a live-cell imaging system (DeltaVision, Applied Precision Inc., Mississauga, ON, USA), which allows automated multi-position time-course fluorescence imaging. To initiate the mating response, various concentrations of α-factor solutions (20 nM–10 μM) were allowed to flow into the inlet hole and subsequently drawn inside the reservoir via the absorption of the solution with a tissue paper at the outlet hole on the opposite site. Using this system, we arbitrarily selected 20 spatial points, each of which covered 49 microwells, under a 60× magnification oil-immersed objective to track cellular responses for 2 h. Differential interference contrast (DIC) and green (GFP)

and red fluorescent (RFP) images were taken of all 20 spatial points every 15 min for a total of 9 time points (0, 15, 30, 45, 60, 75, 90, 105, and 120 min).

Fluorescence image processing

To analyze EPS in terms of the cellular gene expression response, changes in the green and red fluorescence intensities of stimulated cells were measured and analyzed using commercialized image-processing software (ImagePro, Media Cybernetics Inc., Rockville, MD, USA). The average time-lapse green and red fluorescence intensities, lengths of the major and minor eclipse axes, and cell areas were measured using ImagePro scripts. The average red intensity noise and calculated cell area were used for the data filtering of abnormalities (e.g., disappearance or addition of a cell) in a single cell analysis.

Fluorescence-activated cell sorting (FACS) analysis

SH129 cells were grown at 30 °C in YPD medium to A_{600} of approximately 0.5 prior to the FACS experiment. Cells were harvested by centrifugation at 3,000 × g for 5 min and resuspended in 2 mL of the SC medium. The resuspended cells were treated with 10 μM of α-factor and grown at 30 ℃. Samples (200 mL) were harvested at fixed time intervals (15 min) over 2 h and sonicated for 3 s to separate cell clumps. The fluorescence of each sonicated sample was quantitatively determined using a FACSCanto flow cytometer (Becton Dickinson, San Jose, CA, USA) equipped with a 488-nm blue laser. A total of 10,000 cells were recorded per sample.

Yeast cell recovery from microwells

After cells were docked into the microwells and experiment was completed, a single cell was recovered using a microcapillary [TransferTips-R (ICSI); Eppendorf, Hamburg, Germany], a microinjector (InjectMan NI2 and FemtoJet; Eppendorf) and

an inverted microscope (IX7; Olympus Corporation, Tokyo, Japan). First, the PDMS mold was removed, after which a cell was retrieved into the microcapillary from the microwell via capillary action by releasing the pressure from the microinjector. The cell was moved from the microcapillary to the culture plate by reapplying a strong pressure and was allowed to grow into a single colony on the plate.

Repeated stimulus response monitoring

The experimental procedure for the first stimulus was the same as that used for cellular response monitoring, except that the α-factor solutions were removed after a 105-min exposure. The YOC system was filled with the SC medium, until enough time had passed for response inactivation (approximately 240 min after the initial stimulus). At 240 min, the α-factor solution was allowed to flow into the inlet hole for the second stimulation and was removed at 345 min and replaced by the SC medium. The signal inactivation of the second stimulus was observed until 480 min.

Statistical analysis of the experimental data

Correlation coefficient refers to PCC between two expression profiles. EPS is defined as the degree of cell–to-cell variation and is calculated as 1 − APCC, where APCC is the average of PCCs for all possible pairs of expression profiles in the data set. The distance between two expression profiles, x and y, is defined as 1 − PCC (x, y). The degree of fluctuation measures the number of fluctuation points divided by n − 2, where fluctuation points indicate slope-sign changing points and n is the number of sampling time points obtained from the single cell response profile. CAP of an expression profile x stands for PCC between x and the average profile of all expression profiles in the data set. If the expression profiles have similar increasing/decreasing patterns, the CAP value is near one, implying low variance. The signal response value is the total area under the signal response curve. To

distinguish subtypes within the yeast population, signal response grouping was performed by k-means clustering with MATLAB (Mathworks, Inc., Natick, MA, USA).

RESULTS

Microfluidic platform for high-throughput tracking of mating SRPs

The yeast mating pathway is known to transmit signals through the prototypical MAPK pathway consisting of Ste11(MAPKKK)-Ste7(MAPKK)-Fus3(MAPK) along with the scaffold protein Ste5[13, 37, 81]. These four proteins constitute the major components of the mating pathway. Here we examined mating responses for 120-min and at a single-cell level using the YOC system (Figure 14). We monitored SRPs at the level of transcriptional induction. The expression of green fluorescent protein (yGFP) was driven by the pheromone-dependent *Fus1* promoter. A red fluorescent protein (Tdimer2) expression was driven by the constitutively expressed *Gpd1* promoter to detect cells and verify the viability and condition of each cell (Figures 15a, 15b and 16).

The use of YOC system has several advantages[80, 82]. The foremost benefit comes from the combination of quantitative time-lapse fluorescence microscopy and automated image analysis that are used to investigate dynamic events at a single-cell level. Using this platform, we can trace expression profiles in response to pheromone, which results in a vector quantity consisting of magnitude and direction (Figure 15c). In addition, docking of cells into the YOC micro-wells uniformizes the states of cells as shown in a previous study[83]. Cell state heterogeneity is one of the known causes of cell-to-cell variation, and chemicals are often used for cell synchronization. However, as previously noted, the chemicals used for cell synchronization can be harmful, as indicated by increased cell death and decreased responsiveness, while their success rates can differ depending on circumstances[84]. The YOC system used in this study has calculated and uniformly sized wells that only capture round-shaped cells in the G1-phase[85] (Figure 14b). In addition, α-factor induced pheromone-dependent G1 cell cycle arrest further ensures the uniformity of cells captured in the YOC[86]. Moreover, the possibility of cell-to-cell communication that would affect the signal transduction output could be

Figure 14.

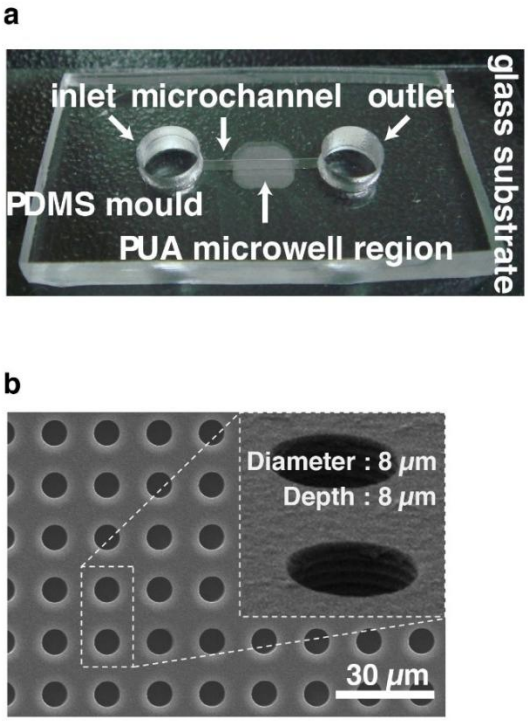
a
inlet
microchannel
outlet
glass substrate
PDMS mould
PUA microwell region
b
Diameter : 8 μm
Depth : 8 μm
30 μm

Figure 14. Image of the YOC system.

(a) Overview of the YOC system with two punched reservoirs and one microfluidic channel. (b) A scanning electron microscope image of the PUA microwell region containing wells with width and depth of 8 μm.

This figure appeared in: Hur, JY. (2011). *Study of stochasticity in MAP kinase signaling using single-cell analyses* (Doctoral dissertation). Seoul National University, Seoul, Korea.

Figure 15.

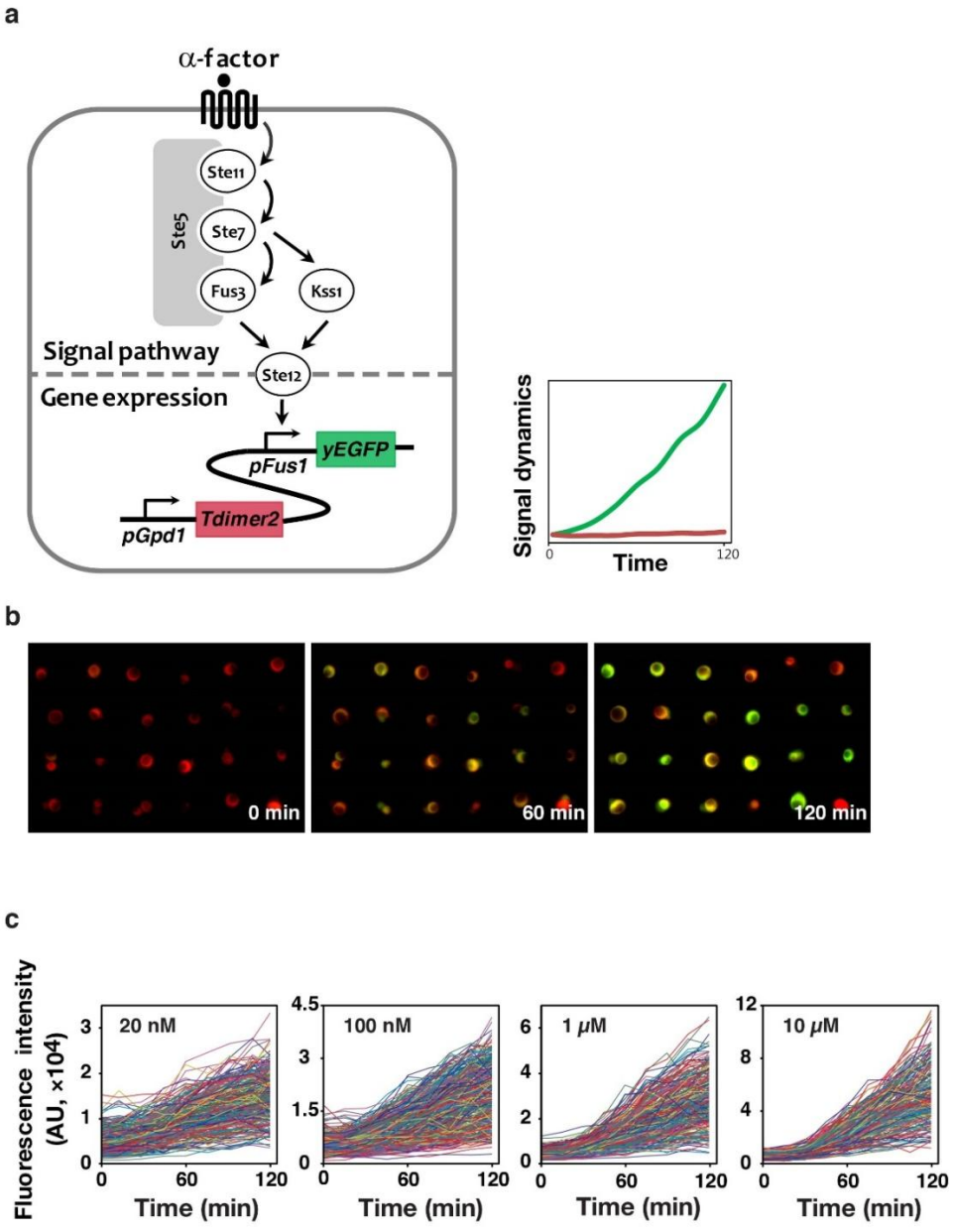
a
α-factor
Ste11
Ste5
Ste7
Fus3
Kss1
Signal pathway
Ste12
Gene expression
yEGFP
pFus1
Tdimer2
pGpd1
Signal dynamics
0
120
Time
b
0 min
60 min
120 min
c
Fluorescence intensity (AU, ×10⁴)
20 nM
100 nM
1 μM
10 μM
Time (min)

Figure 15. A schematic diagram of the mating pathway in *S. cerevisiae* and experimental designs.

(a) The signaling pathway is comprised of the scaffold protein Ste5, three-tier kinases Ste11-Ste7-Fus3 or Kss1, and the transcription factor Ste12. A red fluorescent protein (Tdimer2) is constitutively expressed by the *Gpd1* promoter, and a green fluorescent protein (yEGFP) is expressed by the signal-dependent *Fus1* promoter. (b) Representative images of responses to a mating signal in the YOC system. The mating pheromone induced cellular response in the YOC system is shown as an increase in green fluorescence (yEGFP reporter gene) driven by mating-responsive promoter *Fus1*. SH129 cells were docked in the YOC system and subsequently exposed to 10 μM α-factor through the microfluidic channel. Fluorescent images were taken at 15-min intervals using fluorescence time-lapse microscopy. Before the stimulus, only red fluorescence is detected and as signal transduction continues, the green fluorescence becomes stronger (Extended Data Fig. 2 and Video 1). Representative merged images show a mix of red and green signals at 0, 60, and 120 min. (c) Green fluorescence intensity profiles of cells at different pheromone concentrations. To compare the degree of cell-to-cell variation at various pheromone concentrations, we treated cells with total concentrations of 20 nM, 100 nM, 1 μM, and 10 μM α-factor. Each time-lapse graph represents results from more than 200 cells.

This figure appeared in: Hur, JY. (2011). *Study of stochasticity in MAP kinase signaling using single-cell analyses* (Doctoral dissertation). Seoul National University, Seoul, Korea.

Figure 16.

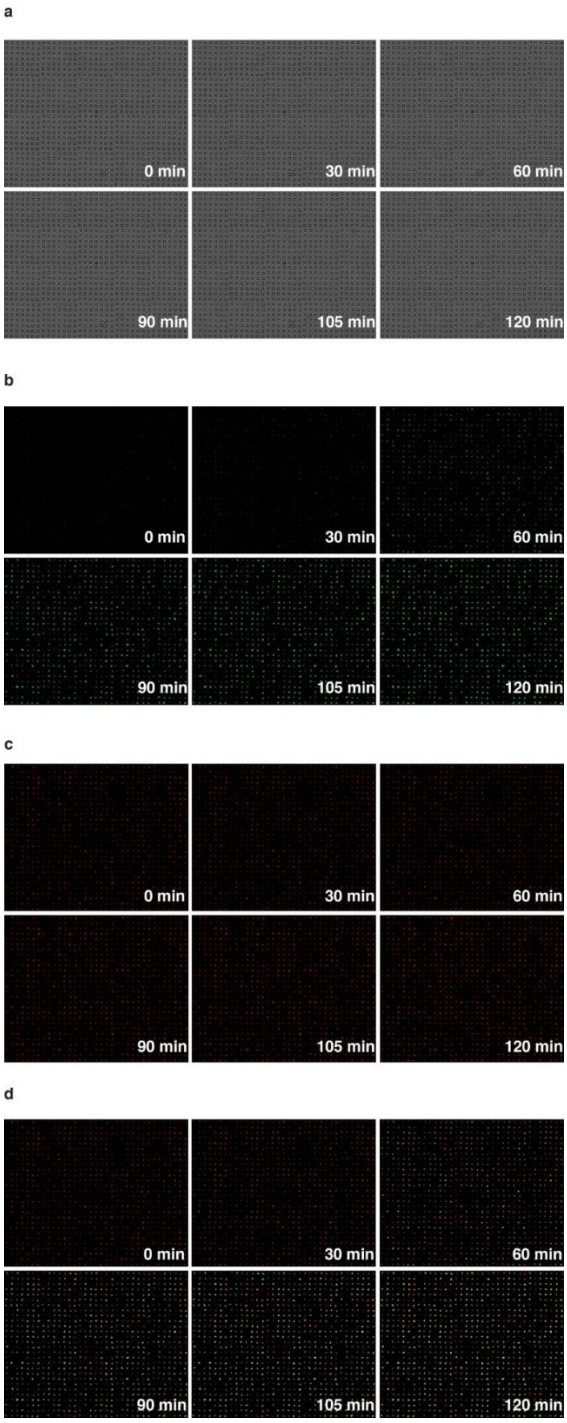
a
0 min
30 min
60 min
90 min
105 min
120 min
b
0 min
30 min
60 min
90 min
105 min
120 min
c
0 min
30 min
60 min
90 min
105 min
120 min
d
0 min
30 min
60 min
90 min
105 min
120 min

Figure 16. Single cell response to the mating signal.

Mating pheromone (α-factor) induced responses. After SH129 cells were docked in YOC, α-factor was flowed into the microfluidic channel and fluorescent images were taken with a time interval of 15 min using fluorescent time-lapse microscopy. Representative microscopic images for 0, 30, 60, 90, 105, and 120 min time points with 10 μM α-factor treatment. Red fluorescent (Tdimer2) is constitutively expressed by *Gpd1* promoter and mating-responsive promoter (*Fus1*) drove the green fluorescent (yEGFP) reporter gene. (a) DIC: bright field images (b) yEGFP: green fluorescent (c) Tdimer2: red fluorescent images (d) Merged images show diverse colors from a mixture of green and red fluorescence.

This figure appeared in: Hur, JY. (2011). *Study of stochasticity in MAP kinase signaling using single-cell analyses* (Doctoral dissertation). Seoul National University, Seoul, Korea.

disregarded while maintaining an environment comparable to that of bulk experiments, as demonstrated by the similarity of the average mating response outputs between the YOC system and bulk experiments. (Figure 17).

Greater EPS under the low-stimulus condition

We used time-traced SRPs to overcome a fragmentary time point-based data evaluations and analyzed these response profiles to determine RPS. To examine RPS and how cells responded to different input strengths, we exposed cells to four different concentrations of α-factor (20 nM, 100 nM, 1 μM, and 10 μM) and monitored the green and red fluorescence expression for 120-min. As expected, p*Gpd1*-red expression did not change over time, whereas p*Fus1*-green intensity increased in response to the pheromone (Figures 15a and 16). We did not find any association between the cell size and green fluorescence intensity or between the red and green fluorescence intensities (Figure 18). These results indicated that neither influenced SRPs of green fluorescence.

A visual inspection of the images clearly showed an increase in response intensity as well as cell-to-cell variability under all four stimulus concentrations (Figures 15b and c). To quantify these variabilities, we defined RPS as the degree of cell-to-cell profile variation, calculated using the following formula: RPS = 1−APCC. The average Pearson correlation coefficient (APCC) denotes the average of the Pearson correlation coefficients (PCCs) between possible pairs of expression profiles in a data set. The APCC of *n* expression profiles is defined as follows:

$$\text{APCC}=\frac{2}{n(n-1)}\sum_{1\le i_1<i_2\le n}\text{PCC between } x_{i_1} \text{ and } x_{i_2},$$

where x_{i_1} and x_{i_2} are different expression profiles in the data set. RPS approaches 1 if the profiles are randomly assigned and approaches 0 if the profiles are similar to each other.

The RPS analysis of red fluorescence data yielded similar values under all

Figure 17.

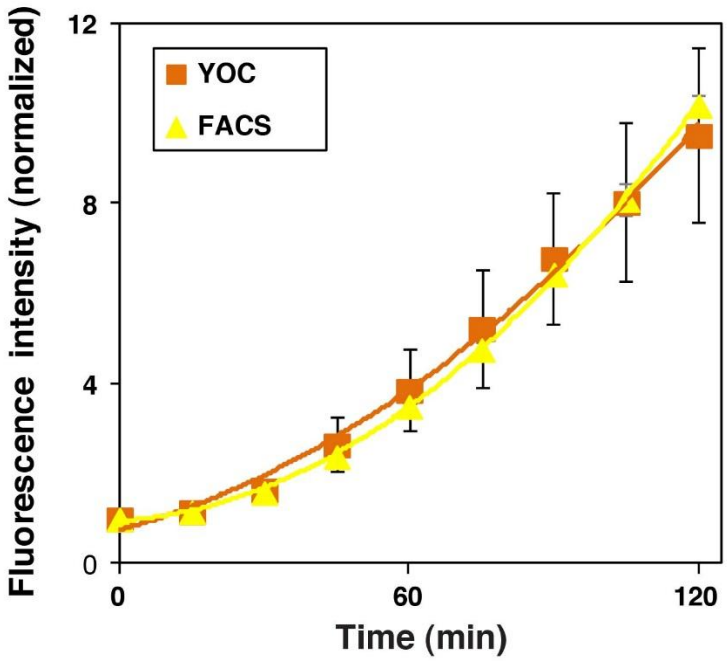
Fluorescence intensity (normalized)
12
8
4
0
YOC
FACS
0
60
120
Time (min)

Figure 17. Comparison of the average signal outputs of the YOC system and bulk experiment system.

Normalized average green fluorescence intensity obtained with the YOC system was similar to that obtained from typical bulk experiments via flow cytometry (e.g., FACS), suggesting that the YOC environment ensures similar conditions with respect to cell viability and proper reactions to mating signals.

This figure appeared in: Hur, JY. (2011). *Study of stochasticity in MAP kinase signaling using single-cell analyses* (Doctoral dissertation). Seoul National University, Seoul, Korea.

Figure 18.

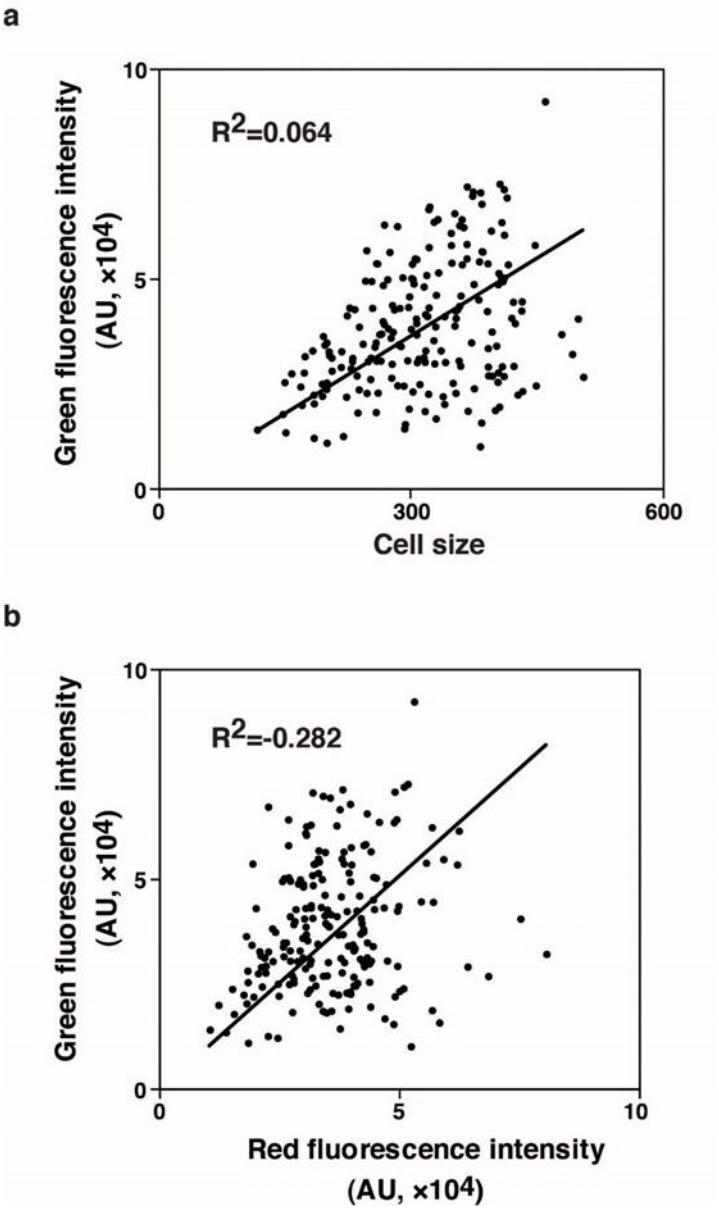
a
10
5
0
0
300
600
Green fluorescence intensity
(AU, ×10⁴)
Cell size
R²=0.064
b
10
5
0
0
5
10
Green fluorescence intensity
(AU, ×10⁴)
Red fluorescence intensity
(AU, ×10⁴)
R²=-0.282

Figure 18. Association of cell size or red fluorescence with signal transduction intensity.

(a) Association of green fluorescence intensity with cell size. Cell size is unrelated to the green fluorescence intensity, which serves as an index of signal transmission. (b) Association of green fluorescence intensity with red fluorescence intensity. Constitutively expressed red fluorescence intensity was unrelated to green fluorescence intensity.

This figure appeared in: Hur, JY. (2011). *Study of stochasticity in MAP kinase signaling using single-cell analyses* (Doctoral dissertation). Seoul National University, Seoul, Korea.

four stimulus concentrations that remained constant throughout the experiments (Figure 19). On the other hand, the RPS analysis of green fluorescence confirmed that it existed at all four stimulus concentrations. However, the RPS level distinctively increased as the strength of stimulation decreased. Specifically, RPS at the lowest stimulus condition was about three-fold higher than that of the highest stimulus condition. These results indicate that RPS is higher under weak stimulation in an isogenic population (Figure 20a).

Moreover, SRPs were sufficiently distinct to allow classification into subtypes using k-means clustering. Once each SRP was fitted into a smooth curve, they were divided into four distinct patterns: rapid-and-continuous-response (blue), rapid-response-and-adaptation (red), slow-response (green) and no-or-random-response (yellow). The rapid-and-continuous-response was the predominant pattern under all four stimulus concentrations. However, a distinctive difference appeared between the low- and high-stimulus conditions. Under the weak condition, SRPs comprised four distinctively divided subtypes, whereas under the strong condition, the rapid-and-continuous response appeared as the general trend, while the frequencies of the other response forms diminished (Figure 20b).

It is important to acknowledge that mating also involves competition. It begins with the detection of the opposite pheromone and the cell's decision to induce a mating response, which can be costly for an individual if the attempt fails. Once the decision is made, the success of mating depends on mutual attraction, led by fusion with the opposite haploid. Therefore, yields a competitive advantage to a quickly responding cell. Distinction in the speed and strength of a signal could arise from differences in the haploid proximity, genetic qualities, or cell states[76, 87, 88]. Since we eliminated those factors, differences in the response initiation suggests that isogenic cells have the capacity to make different decisions.

Another crucial aspect of signal transduction is the deactivation or adaptation process[13, 89]. Two major groups stood out in the clustering of the yeast population: one group continued on to possible success in mating (Figure 20b, blue

Figure 19.

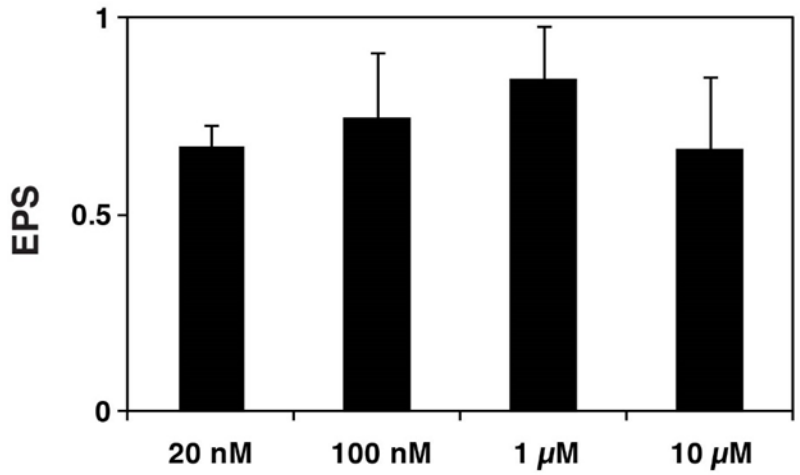

Figure 19. Analysis of EPS via red fluorescence at various stimulation concentrations.

EPS of the red florescence signal at various pheromone concentrations. EPS was very high under all four conditions, suggesting little change in the cell states during the experimental process.

This figure appeared in: Hur, JY. (2011). *Study of stochasticity in MAP kinase signaling using single-cell analyses* (Doctoral dissertation). Seoul National University, Seoul, Korea.

Figure 20.

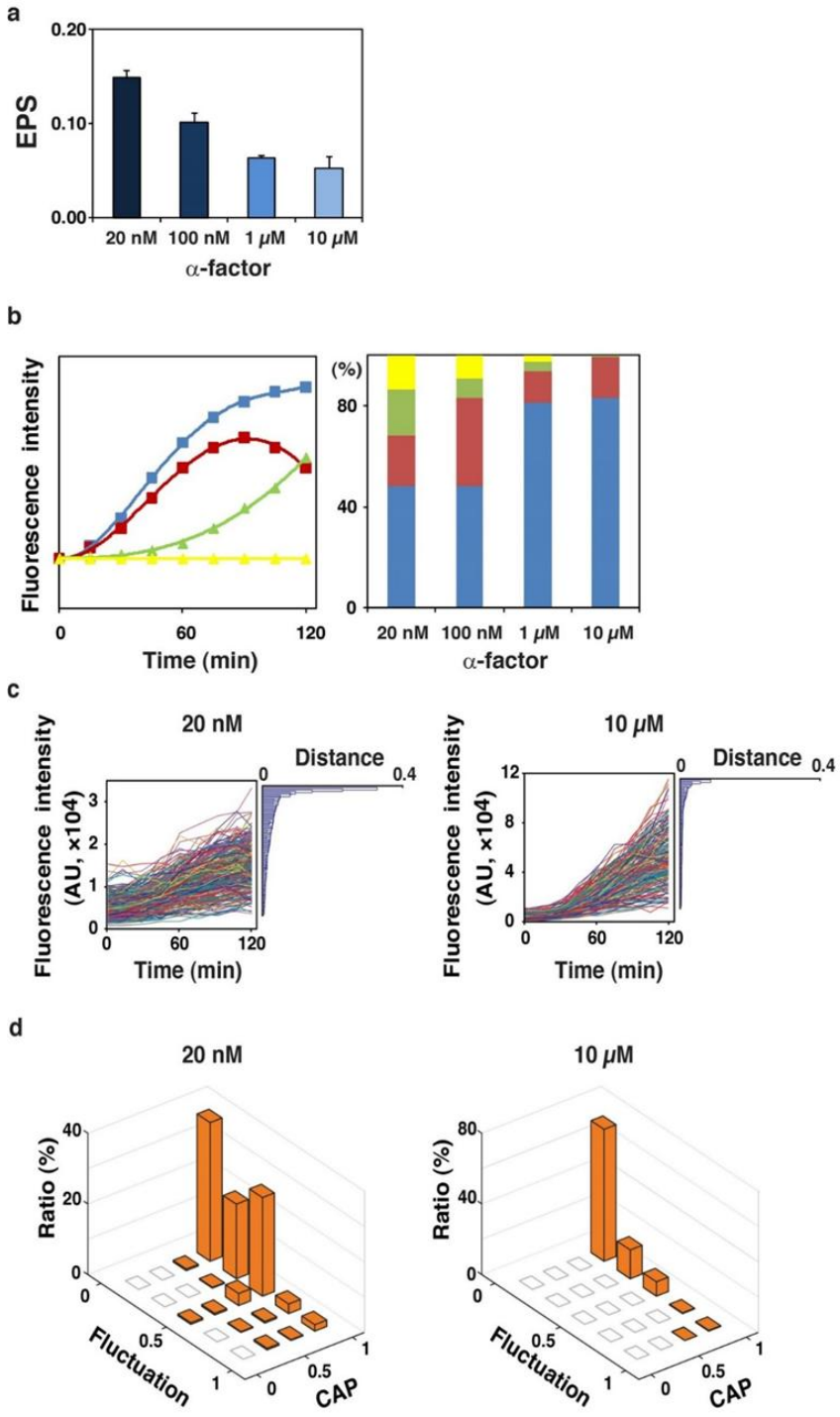
a
EPS
0.20
0.10
0.00
20 nM
100 nM
1 μM
10 μM
α-factor
b
Fluorescence intensity
0
60
120
Time (min)
(%)
80
40
0
20 nM
100 nM
1 μM
10 μM
α-factor
c
20 nM
Distance
0
0.4
Fluorescence intensity (AU, ×104)
3
2
1
0
0
60
120
Time (min)
10 μM
Distance
0
0.4
12
8
4
0
Fluorescence intensity (AU, ×104)
0
60
120
Time (min)
d
20 nM
Ratio (%)
40
20
0
0
0.5
1
Fluctuation
0
0.5
1
CAP
10 μM
Ratio (%)
80
40
0
0
0.5
1
Fluctuation
0
0.5
1
CAP

Figure 20. Analysis of RPS at various stimulation levels.

(a) RPS in the mating signal at various pheromone concentrations. RPS was higher under a low-stimulus condition and lower under a high-stimulus condition. (b) Diverse mating response patterns: rapid and continuous response (blue), rapid response and adaptation (red), slow response (green), and no or random response (yellow). The shapes of the four categorized patterns are shown to the left. To the right, the graph colors demonstrate the representation of the four patterns at different α-factor concentrations. All four patterns are detected under low-stimulus conditions, whereas majority of the cells exhibit the rapid and continuous response pattern (blue) as the stimulus becomes stronger. (c) The dendrogram comparison of variation under low- and high-stimulus conditions. This dendrogram was constructed using 100 randomly chosen expression profiles from each dataset (20 nM or 10 μM) via hierarchical clustering based on the pair-wise distances. Cells under low stimulus exhibit a higher distance value (near 0.4). (d) Distribution of cells with respect to the 'degree of fluctuation' and 'correlation with average profile (CAP)'. Cells under low-stimulus conditions are more widely dispersed than those under high-stimulus conditions.

This figure appeared in: Hur, JY. (2011). *Study of stochasticity in MAP kinase signaling using single-cell analyses* (Doctoral dissertation). Seoul National University, Seoul, Korea.

and green) and the other group admitted early failure and initiated the deactivation process (Figure 20b, red). Because haploid cells that fail to mate eventually initiate signaling pathway deactivation and resume vegetative growth, the timing of deactivation is important to cell's fate[87, 88]. In particular, cells exhibited a clear distinction between early adapters and endurers not only in the low-stimulus condition where RPS was high but also in the high-stimulus condition where the population responses were almost uniform (Figure 20b).

For a further understanding of RPS under the low- versus high-stimulus conditions, we performed hierarchical clustering based on the correlation distance between expression profiles. Cells exposed to low-stimulus had higher pairwise distances than compared to those exposed to high-stimulus, which had small or near zero pairwise distances implying low RPS (Figure 20c). In addition, analyses of the 'degree of fluctuation' and 'correlation with the average response profile (CAP)' revealed marked differences in the distribution of SRPs between the low- and high-stimulus conditions. Under the low-stimulus condition, majority of the cells exhibited a high degree of fluctuation, low correlation with the average response profile, or both. In contrast, under high-stimulus, most cells exhibited no fluctuation and high CAP values (Figure 20d). Multiple analyses consistently demonstrated a large RPS under the low-stimulus condition, despite a uniform genetic background, cell state and environment.

RPS originates from the MAPK pathway

The observed signaling process could be divided into two parts: from the receptor to the activation of transcription factor Ste12 and from there to the induction of p*Fus1*-yGFP transcription. Ste12 acts as the midpoint and accordingly receives the signal transmitted from the pathway and subsequently activates genes involved in the shmooing and merging of cells. It is well established that the overexpression of Ste12 alone, without a stimulus, can induce α-factor-induced genes, including *Fus1*[32]. If RPS originated from expressional noise depended on the

transcriptional machinery of mating-related genes, we would observe greater RPS with Ste12 overexpression. Previous studies have shown high level of dispersion stochasticity and suggested that expressional noise is the main cause of stochasticity[54, 58, 64]. In our experiments, a conventional analysis of the dispersion of expression at 120-min also indicated high stochasticity (data not shown).

On the contrary, RPS resulting from a Ste12 overexpression was found to be relatively low, similar to the value under the high-stimulus condition (Figure 21a). It seems that the low RPS observed under the high-stimulus condition originated from the expressional noise downstream of Ste12. More importantly, majority of RPS, especially under the low-stimulus condition, appeared to originate from the signal flow though the MAPK pathway.

MAPK abundance has the greatest influence on RPS

Having shown that RPS exists among SRPs, we wondered which component of the mating pathway would contribute the most to response diversification. We over-expressed Ste11, Ste7, Fus3 or Ste5, which are the four key components of the classical three-tier cascade, and subsequently observed changes in RPS. The singular overexpression of the three kinases or scaffold protein induced similar response strengths in all four constructs (Figure 22). In all constructs, while signal transduction intensities were similar, SRPs were noticeably different, leading to increased RPS (Figures 21b and c). Protein overexpression increased the range of variation in the ability of cells to express proteins, leading to higher stochasticity in protein numbers. This outcome was to be expected from various previous works that demonstrated the existence of cellular noise in both prokaryotes and eukaryotes[55, 64, 90-92].

The difference in the increase of RPS emerged as the prominent finding. The overexpression of both Ste11 and Fus3 displayed increase in RPS under the high-stimulus condition, whereas in the low-stimulus condition, only Fus3 overexpression distinctively induced the greatest increase in RPS (Figures 21b and

Figure 21.

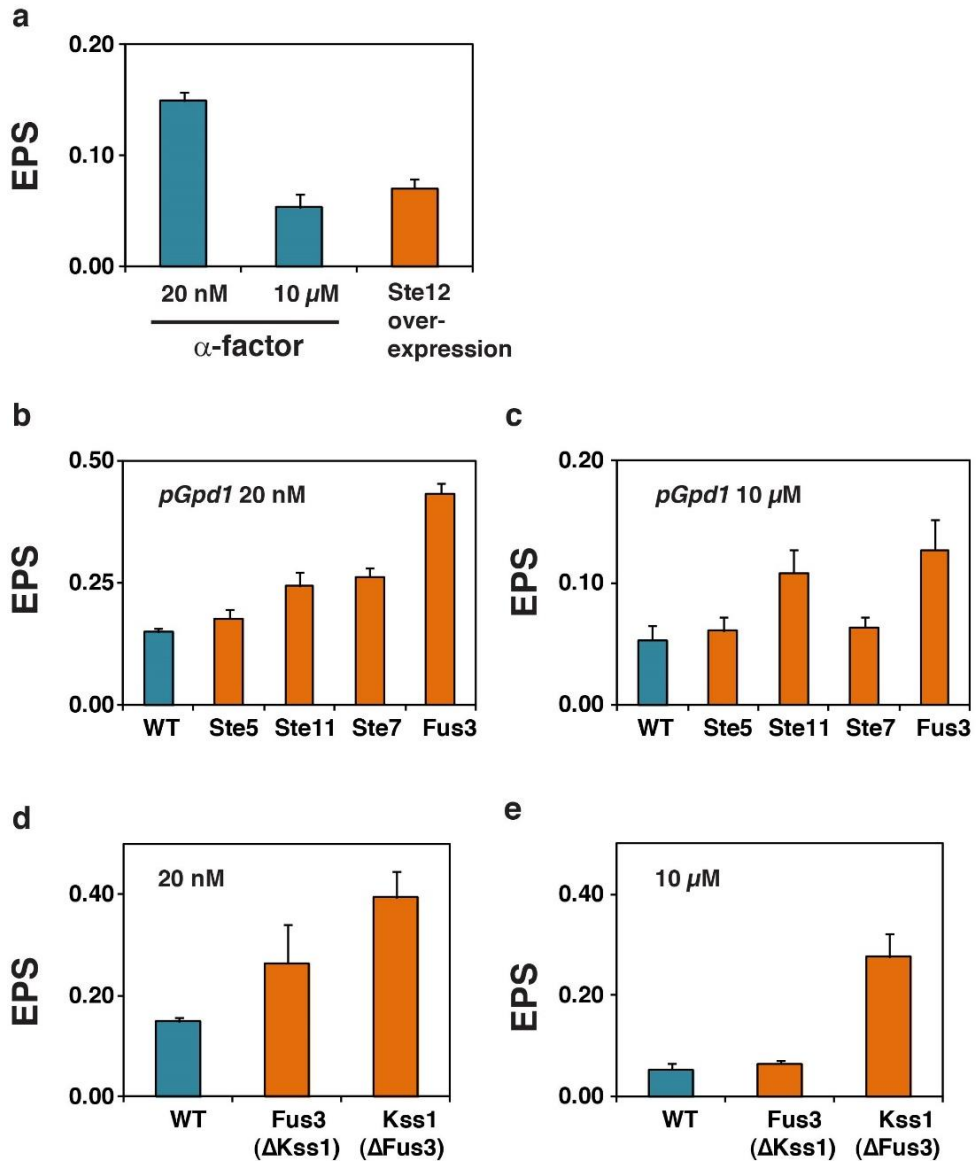
a
EPS
0.20
0.10
0.00
20 nM
10 μM
α-factor
Ste12
over-
expression
b
EPS
0.50
0.25
0.00
pGpd1 20 nM
WT
Ste5
Ste11
Ste7
Fus3
c
EPS
0.20
0.10
0.00
pGpd1 10 μM
WT
Ste5
Ste11
Ste7
Fus3
d
EPS
0.40
0.20
0.00
20 nM
WT
Fus3
(ΔKss1)
Kss1
(ΔFus3)
e
EPS
0.40
0.20
0.00
10 μM
WT
Fus3
(ΔKss1)
Kss1
(ΔFus3)

Figure 21. Source of RPS.

(a) RPS of gene expression. In the case of Ste12 overexpression, the experimental procedures were the same except that 2% galactose was flowed into the microfluidic channel, rather than α-factor. Ste12 overexpression induces the expression of α-factor-responsive genes. RPS of Ste12 overexpression was calculated from fluorescent intensity data and compared with α-factor induction data. RPS of Ste12 overexpression was similar to the values obtained from a 10 μM α-factor experiment and demonstrated relatively low stochasticity. (b and c) Effects of changes in the abundance of MAPK pathway components on RPS. SH129 cells were transformed with vectors to induce the overexpression of Ste5, Ste11, Ste7, or Fus3. (b) Under low-stimulus conditions, RPS increased in all cases of overexpression. (c) Fus3 overexpression stands out with an approximate three-fold increase in the stochastic value with low stimulus and a slight increase with high stimulus. (d and e) Stochasticity of the ΔKss1 and ΔFus3 strains. Cells with Fus3 (ΔKss1) and Kss1 (ΔFus3) overexpression were treated with α-factor at (d) 20 nM or (e) 10 μM. RPS increased in the Fus3 (ΔKss1) strain and to a greater extent in the Kss1 (ΔFus3) strain compared to values from the wild-type (WT) strain.

This figure appeared in: Hur, JY. (2011). *Study of stochasticity in MAP kinase signaling using single-cell analyses* (Doctoral dissertation). Seoul National University, Seoul, Korea.

Figure 22.

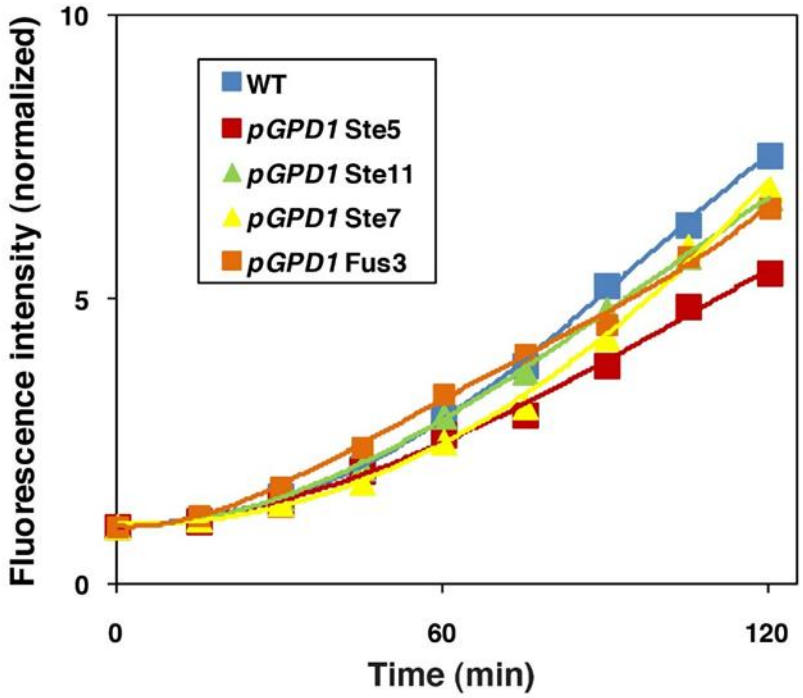
Fluorescence intensity (normalized)
10
5
0
0
60
120
Time (min)
WT
pGPD1 Ste5
pGPD1 Ste11
pGPD1 Ste7
pGPD1 Fus3

Figure 22. Average signal transduction in p*Gpd1*-overexpressing and wild-type cells.

The average fluorescence intensity was calculated from approximately 200 individual cells in the YOC system that had been exposed to 10 μM α-factor. The average fluorescence intensities were normalized to the value 1 at 0 min time-point for the purpose of comparison. All overexpression constructs under the control of the *Gpd1* promoter exhibited similar average signal transduction intensities to those of the average wild-type value.

This figure appeared in: Hur, JY. (2011). *Study of stochasticity in MAP kinase signaling using single-cell analyses* (Doctoral dissertation). Seoul National University, Seoul, Korea.

c). In a further analysis involving the overexpression of three kinases at two different levels, the results corresponded to a large increase in RPS under both low- and high-stimulus conditions only when Fus3 was over-expressed (Figures 23a and b). Distinctively, the MAPK Fus3 expression appeared to have the greatest influence on RPS. What makes the mating pathway more interesting is the existence of another MAPK, Kss1[37]. Kss1, a main signaling component of the invasive-filamentous growth pathway, also plays a part in transmitting signals in response to pheromones[93]. Within the mating pathway, Fus3 appears to mediate slow and ultrasensitive responses, whereas Kss1 appears to mediate rapid and graded responses[94]. Therefore, we further investigated the different mechanisms by which Fus3 and Kss1 contribute to the response diversity by deleting one kinase at a time. The results revealed that the deletion of Fus3 increased RPS more markedly under both stimulus conditions, indicating that signal flow through Fus3 was preferred for a more stable signal transmission. (Figures 21d and e).

Non-genetic and inherent RPS of the MAPK signaling pathway

To determine whether SRP is a non-genetic but distinctive characteristic, we evaluated the inheritability of RPS. The existence of distinct profiles in a clonal population exposed to a uniform environment suggests that the signal output strength could be determined by non-genetic but inheritable factors. We recovered the brightest and dimmest cells from the YOC after our initial experiment to determine whether these cells would preserve their traits and pass on to the next generation (Figure 24). After multiple rounds of growths in separate batch cultures, daughter cells were subjected to the same experiment. Daughter cells of the brightest and dimmest cells, when exposed to low- or high-stimulus conditions, exhibited RPS values nearly identical to those observed in the initial experiment, regardless of response intensities of their mother cells (Figures 25a, b and c). These results showed that the output of each cell is not inherited and that RPS in the yeast MAPK pathway arises from non-genetic and inherent factors.

Figure 23.

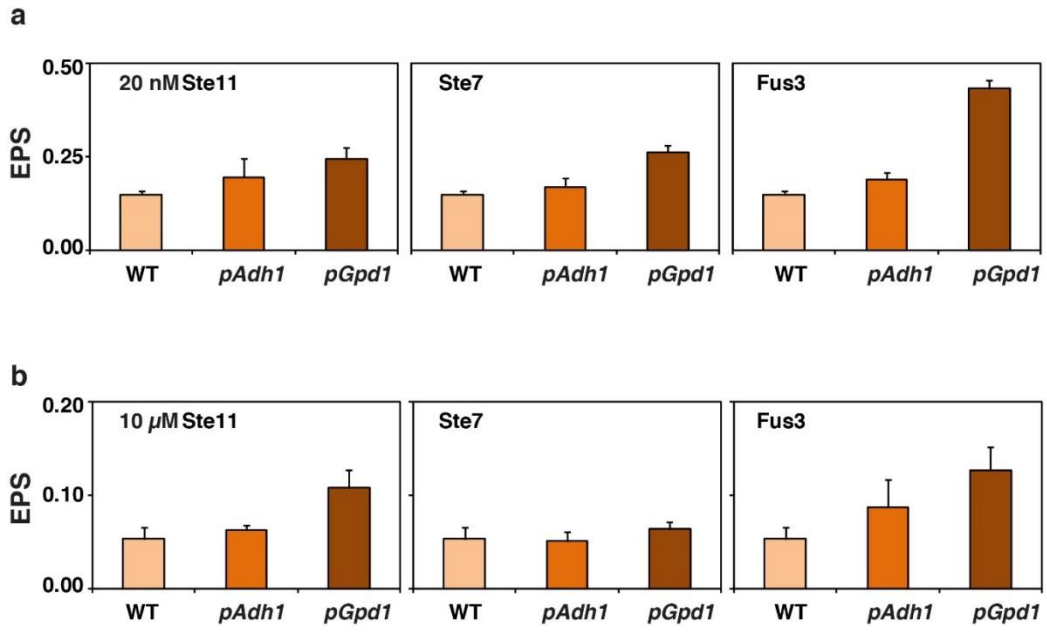
a
EPS
0.50
0.25
0.00
20 nM Ste11
Ste7
Fus3
WT
pAdh1
pGpd1
b
EPS
0.20
0.10
0.00
10 μM Ste11
Ste7
Fus3
WT
pAdh1
pGpd1

Figure 23. Effects of the overexpression of MAPK pathway kinases on EPS.

Kinase protein expression was increased via stronger promoters (*Adh1* or *Gpd1*) to be compared to endogenous promoter-induced expression. (a) Calculated EPS under the low-stimulus condition (20 nM α-factor). (b) Calculated EPS under the high-stimulus condition (10 μM α-factor). In all cases, stochasticity increases as abundance increases, and a notably stronger variation is observed with Fus3 overexpression.

This figure appeared in: Hur, JY. (2011). *Study of stochasticity in MAP kinase signaling using single-cell analyses* (Doctoral dissertation). Seoul National University, Seoul, Korea.

Figure 24.

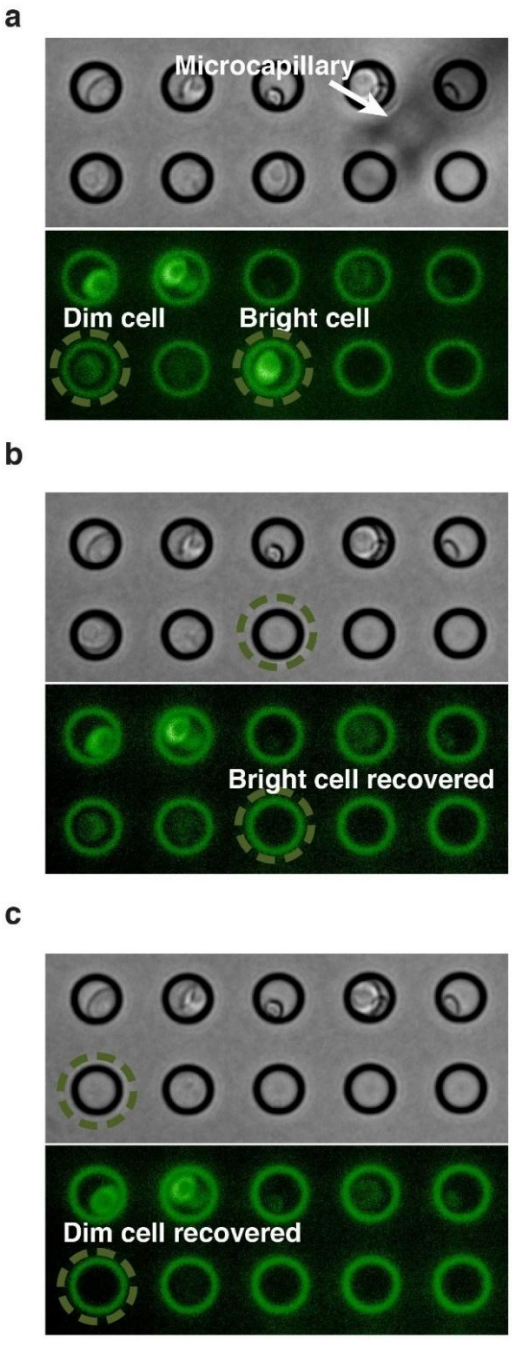
a
Microcapillary
Dim cell
Bright cell
b
Bright cell recovered
c
Dim cell recovered

Figure 24. Yeast cell recovery from YOC microwells.

(a) A bright cell and a dim cell in microwells. Cells docked in microwells were recovered using a microcapillary, a microinjector, and an inverted microscope. (b, c) Recovery of bright and dim cells. For cell recovery, the PDMS mold was removed from the YOC system containing docked cells. Next, the cell was retrieved from the microwell in the microcapillary via capillary action by releasing pressure from the microinjector.

Figure 25.

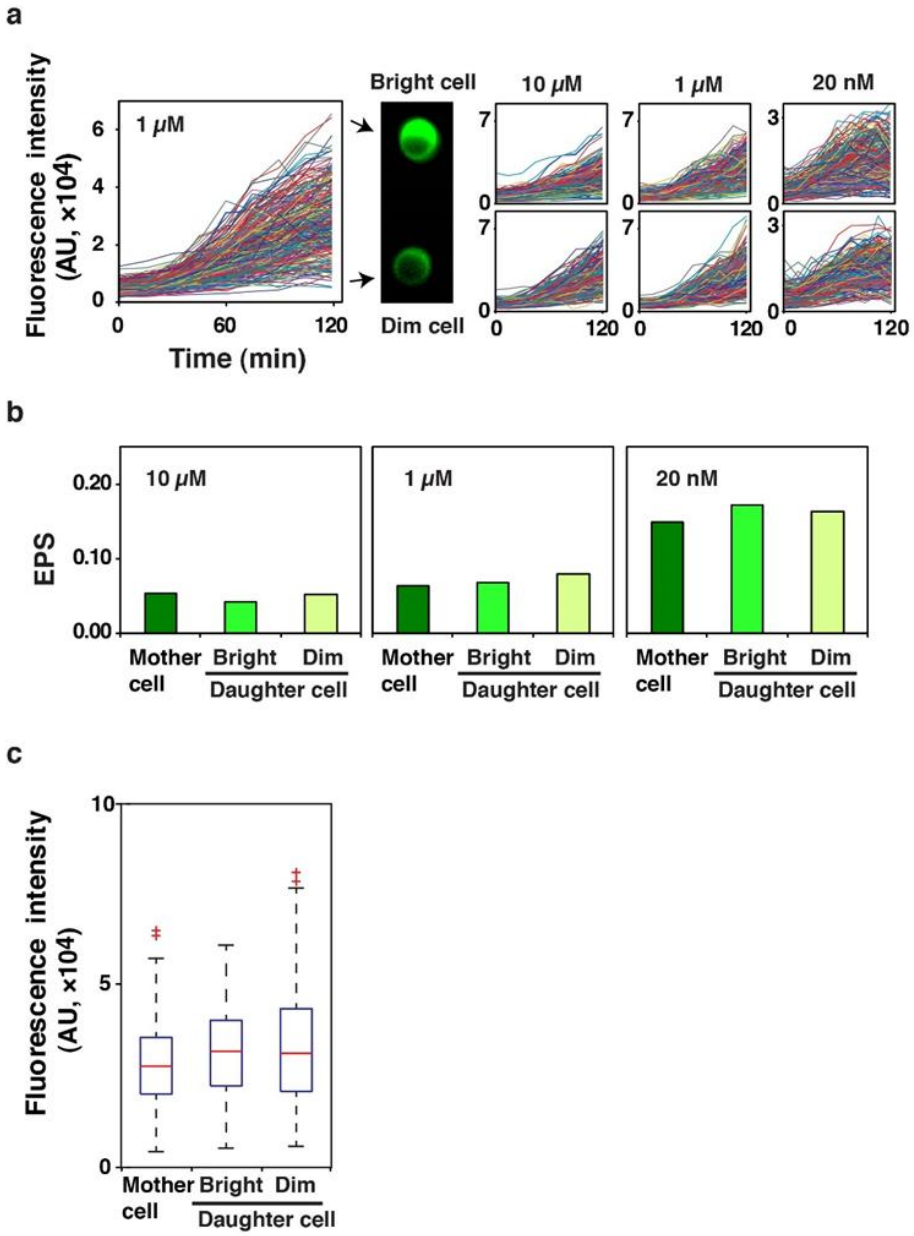
a
Fluorescence intensity (AU, ×104)
1 μM
Time (min)
Bright cell
Dim cell
10 μM
1 μM
20 nM
b
EPS
10 μM
1 μM
20 nM
Mother cell
Bright
Dim
Daughter cell
c
Fluorescence intensity (AU, ×104)
Mother cell
Bright
Dim
Daughter cell

Figure 25. Test of inheritability.

(a) Green fluorescence intensities of the mother and daughter cells. Particularly bright and dim cells were selected from the first group of cells (mother cells) exposed to 1 μM α-factor. Selected daughter cells (bright and dim) were subjected to mating response tests with 20 nM, 1 μM or 10 μM α-factor. Plotting of the fluorescence intensity values displays the diversity among cell responses and visually demonstrates similar levels of diversity in the responses of the mother cells and both types of daughter cells. (b) RPS comparison of a mother cell and recovered daughter cells. A dim cell and a bright cell were recovered from the initial YOC experiment and were separately seeded. After batch cultivation, these cells were subjected to two separate YOC experiments. At all tested stimulus concentrations (20 nM, 1 μM, or 10 μM), both type of cells displayed similar RPS fluxes as the mother cell. (c) The box plot shows green fluorescence intensity distributions at 120 min under a 1 μm α-factor concentration condition. The mother cell comprises all cells from the first experiment. Daughter cell refers to either the bright or dim cell recovered from the YOC system, grown in a batch culture, and subjected to a second round of experiments on the YOC system. The RPS distributions, indicated by green fluorescence, were similar in the mother cells and both types of daughter cells.

For further characterization, we examined whether repeated exposure to stimuli would induce a similar response. Accordingly, cells were exposed to repeating stimuli separated by sufficient time intervals to allow for deactivation. The average signal transduction intensities in response to the first and second pheromone exposures were almost identical (Figure 26a). Also, a comparison of the two SRPs in an individual cell did not show a strong correlation (Figures 26b and c). Separate RPS analyses of the first and second responses, along with a combined analysis of both responses, all yielded similar stochastic values (Figure 26d). Together, these data suggest that a cell could exhibit the same response intensity to both stimuli, strongly respond to the first stimulus and weakly respond to the second stimulus, or vice versa. This finding demonstrates that RPS resulting from signal transduction leads a cell to make separate decisions with each exposure to a stimulus, even under the same environmental conditions. Therefore, SRP is not a result of a non-genetic but uniquely implanted trait, and the initial response pattern is not memorized by the cell. RPS appears to be an inherent factor possessed by all yeasts that confers the ability to respond differently under a weak stimulus condition.

In addition, the average response values should not be over-looked on both occasions as they stay about the same throughout the mother-daughter and repeated stimuli experiments. While we highlighted the diversity aspect of isogenic yeasts as an individual, yeasts as a population is putting out a consistent average output being a reliable responder to the environmental cue.

Figure 26.

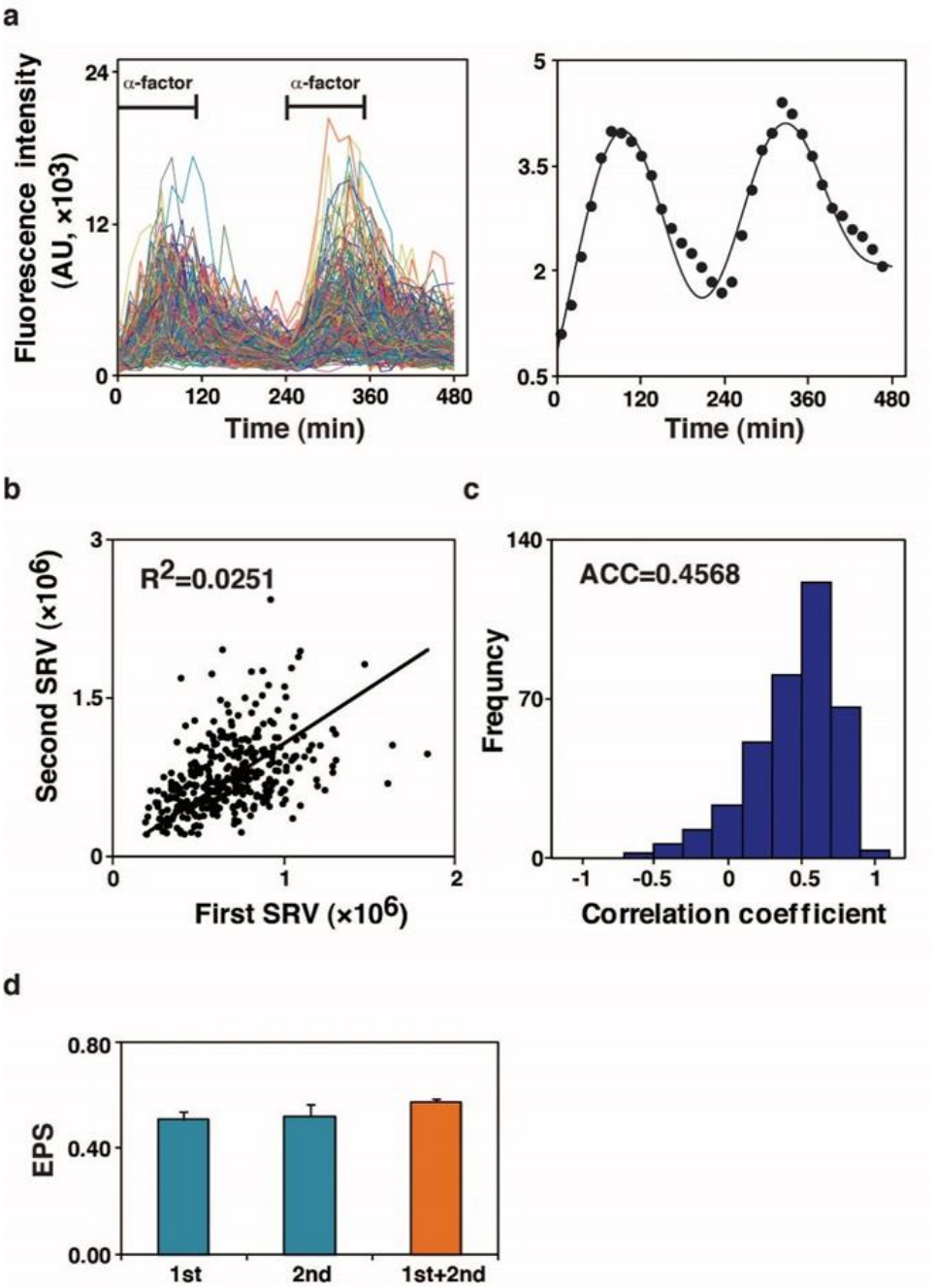
a
Fluorescence intensity (AU, ×103)
α-factor
α-factor
Time (min)
Time (min)
b
Second SRV (×10^6)
R^2=0.0251
First SRV (×10^6)
c
Frequncy
ACC=0.4568
Correlation coefficient
d
EPS
1st
2nd
1st+2nd

Figure 26. Test of repeatability.

(a) Mating signal response to repetitive stimuli. The graph displays the green fluorescence intensities of approximately 400 individual cells subjected to two cycles of 1 μM α-factor stimulation. The first and second rounds of stimuli were applied from 0 min to 105 min and from 240 min to 345 min, respectively. After each stimulus, cells were left without stimulus for more than 120 min to allow the full inactivation of signal transmission. The graph to the right displays the average mating response pattern to repeated stimulation. The average curve shows similar fluorescence intensity levels between the first and second stimulations. (b) Correlation between the mating responses of the first signal response value (SRV) and the second SRV. Plotting the two responses did not reveal a strong correlation. (c) Correlation coefficients of the first and second responses. Correlation coefficient values of the first and second responses range from –0.5 to 1, with an average value of 0.4568. (d) RPS values of the first, second, and both responses. RPS calculations yielded similar stochastic variations for the first, second, and both stimulations as a whole.

DISCUSSION

We performed a time-traceable single-cell analysis and demonstrated the existence of RPS in the mating response of *S. cerevisiae*. The mating pathway is a signal transduction pathway that governs the cell fate decision-making system. In a natural environment, yeast cells would likely belong to a population that undergoes clonal reproduction and intratetrad mating while being exposed to various chemicals including different concentration of pheromones. On sensing a mating signal, yeasts determine whether the opposite haploid is in close proximity and decide within 2 min whether the energy-consuming process of mating should be initiated[95]. When the signal is strong, cells act in coherence by responding quickly and continuously. Naturally, yeasts face the dilemma of 'to continue reproduction' or 'to mate despite the uncertainty' when the signal is ambiguous. If all the clonal cells in such position acted on the same decision, the population could potentially die out in response to sudden environmental changes or competition. However, nature appears to have stipulated isogenic diversity, working at a level that allows organisms to increase their fitness among cells growing in the same environment.

We discovered four distinctive responses to low-pheromone stimulation that differed with respect to speed and duration. Rapid-responding cells will be the first to successfully mate if the stimulus was indeed produced by an opposite haploid in close proximity. The group of yeast cells that undergo deactivation earlier than others might be saving energy for another mating opportunity. On the other hand, slow-responding cells would likely lose a competition to the rapid-responding cells but might ultimately mate if the rapid-responding cell in question also underwent an early deactivation. Lastly, cells that do not respond at all appear to have ignored this mating opportunity. Previous observations of the coexistence of budding, shmooing, and no response within a pool of yeast also support differences in SRPs[96]. Additionally, as the yeast genome is known to be stable in the states of vegetative growth and meiosis, the possibility that yeast cells would accumulate mutation during the experiment is extremely low[97].

Through a further investigation of the mechanism driving these variations, we found that signal transduction through the MAPK pathway contributes more to RPS than the gene expression noise. RPS generated during signal transduction would confer a time advantage, relative to noise originating from more time consuming gene expressions. Consequently, organisms could quickly adapt to a rapidly changing environment without altering gene expression, mutation or sexual reproduction. Another advantageous feature of RPS is its inherent flexibility. A comparison between mother and daughter cells revealed that the mothers' characteristics were not passed to daughters as daughter cells of different mother cells exhibited RPS levels similar to those in the original population. Previous studies have also demonstrated, either theoretically or experimentally, the beneficial aspect of stochasticity in terms of creating phenotype heterogeneity[70-72, 98-104]. Some theoretical studies suggested that a stochastic phenotype transition allows a faster growth rate in a fluctuating environment[99, 100] and bacterial studies have shown similar finding with regards to survival after antibiotics treatment[102-104]. These data demonstrate that what may seem like a random variation could instead be a source of diversification for an isogenic population.

In this study, we presented evidence that yeast cells possess an inherent capacity for stochasticity even under identical environments thus conferring a survival advantage against circumstantial changes. Regarding heterogeneity, bulk-scale measurements can be problematic as these only report a single average value from all cells in the population. However, the unexpected aspect of RPS is the inherent and not inheritable trait, which makes the identification of subpopulations via single cell analysis insufficient or unnecessary. Rather, the classical bulk-scale measurement experiments seem more adequate for the purpose of identifying responses to a specific condition or environmental change.

Our understanding of causes and functional consequences of variation in biological systems is vague, mainly because such behaviors are unpredictable and difficult to define. Therefore, when measuring quantities that change over time, as in the case of gene expression profiles in response to stimuli, it is important to

consider the dynamic response, as demonstrated in this study. Our microfluidic platform allows high-throughput single-cell tracking for various signal transduction pathways and stimuli, thus allowing studies on diversity as well as its causes and consequences. A broader and deeper understanding of the diversity observed among cells with the same genetic background will allow us to learn more about an organism's intricate balance between diversity in the face of uncertainty versus coherency in the face of certainty and thus facilitate predictions regarding stochastic behaviors.

Table 1. Strains used in this study

Strain	Description
RB206	*MAT***a**, *kss1::KanR, mfa2:: pFus1-LacZ, his3, trp1, leu2, ura3*
RB207	*MAT***a**, *kss1::KanR, ste5::Leu2, mfa2:: pFus1-LacZ, his3, trp1, leu2, ura3*
RB210	*MAT***a**, *fus3::KanR, kss1::NatR, mfa2::pFus1-LacZ, his3, trp1, leu2, ura3*
RB212	*MAT***a**, *fus3::KanR, kss1::NatR, ste7::His3, mfa2::pFus1-LacZ, his3, trp1, leu2, ura3*
SH018	*MAT***a**, *ppq1::His5, mfa::Fus1-LacZ, leu2, trp1, his3*
SH129	*MAT***a**, *fus1::yEGFP-SpHIS5, gpd1::Tdimer2-CaURA3* on SO992
SH130	*MAT***a**, *fus1::yEGFP-SpHIS5, stl1::Tdimer2-CaURA3*on SO992
SH133	*MAT***a**, *fus1::yEGFP-CLN2(PEST)-His3MX6, gpd1::Tdimer2-CaURA3*on SO992
SH152	*MAT***a**, *kss1::KanR, ste7::His3, mfa2::pFus1-LacZ, his3, trp1, leu2, ura3*
SH153	*MAT***a**, *kss1::KanR, ste11::His3, mfa2::pFus1-LacZ, his3, trp1, leu2, ura3*
SH167	*MAT***a**, *kss1::KanR, fus3::Fus3-fluc-His, mfa2:: pFus1-LacZ, his3, trp1, leu2, ura3*
SH176	*MAT***a**, *kss1::KanR, ste7::His3, Ste11::Ura3, mfa2::pFus1-LacZ, his3, trp1, leu2, ura3*
SH177	*MAT***a**, *fus1::yEGFP-SpHIS5, gpd1::Tdimer2-CaURA3, kss1::Trp1* on SO992
SH178	*MAT***a**, *fus1::yEGFP-SpHIS5, gpd1::Tdimer2-CaURA3, fus3::Trp1* on SO992
SH179	*MAT***a**, *fus3::KanR, kss1::NatR, Ste11::Ura3, mfa2::pFus1-LacZ, his3, trp1, leu2, ura3*
SH202	*MAT***a**, *kss1::KanR, ste11::Ste11-fluc-Ura, mfa2:: pFus1-LacZ, his3, trp1, leu2, ura3*
SH203	*MAT***a**, *kss1::KanR, ste7::Ste7-fluc-Ura, mfa2:: pFus1-LacZ, his3, trp1, leu2, ura3*
SH204	*MAT***a**, *kss1::KanR, ste5::Ste5-fluc-Ura, mfa2:: pFus1-LacZ, his3, trp1, leu2, ura3*

Table 2. Plasmids used in this study

Plasmid	Parent vector	Promoter	Description
pSH1277	pRS314	Gal	Ste12
pSH1286	pRS316	Ste11	Ste11-fluc
pSH1288	pRS316	Ste11	Flag-fs-Ste11-fluc
pSH1291	pRS314	Ste7	Ste7-fluc
pSH1293	pRS314	Ste7	Flag-fs-Ste7-fluc
pSH1296	pRS314	Fus3	Fus3-fluc
pSH1298	pRS314	Fus3	Flag-fs-Fus3-fluc
pSH1526	pRS314	Fus3	Fus3
pSH1538	pRS424	Ste11	Ste11
pSH1539	pRS424	Ste7	Ste7
pSH1540	pRS426	Fus3	Fus3-fluc
pSH1600	pRS314	Fus3	Flag-fs-Fus3-fluc
pSH1601	pRS426	Fus3	Fus3
pSH1617	pRS314	Ste11	Ste11
pSH1618	pRS314	Ste7	Ste7
pSH1636	pRS314	Fus3	fs-Fus3
pSH1638	pRS314	Fus3	fs-in-Fus3
pSH1639	pRS314	Ste11	fs-ste11
pSH1641	pRS314	Ste11	fs-in-Ste11
pSH1642	pRS314	Ste7	fs-Ste7
pSH1644	pRS314	Ste7	fs-in-Ste7
pSH1698	pRS424	Ste7	Ste7-fluc
pSH1948	pRS316	Adh1	Ste11-fluc
pSH1949	pRS314	Tef2	Ste11-fluc
pSH1951	pRS314	Adh1	Ste7-fluc
pSH1952	pRS314	Tef2	Ste7-fluc
pSH1954	pRS314	Adh1	Fus3-fluc
pSH1955	pRS314	Tef2	Fus3-fluc
pSH1957	pRS314	Adh1	Ste11

pSH1958	pRS314	Tef2	Ste11
pSH1960	pRS314	Adh1	Ste7
pSH1961	pRS314	Tef2	Ste7
pSH1963	pRS314	Adh1	Fus3
pSH1964	pRS314	Tef2	Fus3
pSH2007	pRS424	Ste11	Ste11-fluc
pSH2011	pRS314	Tef2	Ste5-fluc
pSH2012	pRS314	Adh1	Ste5-fluc
pSH2013	pRS424	Ste5	Ste5-fluc
pSH2014	pRS314	Ste5	Ste5-fluc
pSH2015	pRS314	Ste5	fs-in-Ste5-fluc
pSH2016	pRS314	Ste5	fs-Ste5-fluc
pSH2017	pRS314	Tef2	Ste5
pSH2018	pRS314	Adh1	Ste5
pSH2019	pRS424	Ste5	Ste5
pSH2111	pRS314	Adh1	Ste11-fluc
pSH2112	pRS314	Ste11	Ste11-fluc
pSH2113	pRS314	Ste11	flag-fs-Ste11-fluc
pSH2114	pRS424	Fus3	flag-Fus3-fluc
pSH2316	pRS314	Ste11	fs-in-Ste11-fluc
pSH2317	pRS314	Ste7	fs-in-Ste7-fluc
pSH2468	pRS314	Ste5	Ste5
pSH2469	pRS314	Ste5	fs-in-Ste5
pSH2470	pRS314	Ste5	fs-Ste5
pSH2574	pRS315	Fus1	EGFP
pSH2575	pRS313	Fus1	EGFP
pSH2576	pRS315	Tef2	Fus3
pSH2577	pRS315	Adh1	Fus3
pSH2578	pRS315	Fus3	Fus3
pSH2579	pRS315	Fus3	fs-Fus3
pSH2580	pRS315	Fus3	fs-in-Fus3
pSH2581	pRS315	Fus3	Fus3
pSH2583	pRS315	Tef2	Ste11

pSH2584	pRS315	Adh1	Ste11
pSH2585	pRS425	Ste11	Ste11
pSH2586	pRS315	Ste11	Ste11
pSH2587	pRS315	Ste11	fs-Ste11
pSH2588	pRS315	Ste11	fs-in-Ste11
pSH2672	pRS315	Tef2	Ste7
pSH2673	pRS315	Adh1	Ste7
pSH2674	pRS425	Ste7	Ste7
pSH2675	pRS315	Ste7	Ste7
pSH2676	pRS315	Ste7	fs-Ste7
pSH2677	pRS315	Ste7	fs-in-Ste7
pRS313 is a low-copy yeast vector (CEN/ARS, HIS3)			
pRS314 is a low-copy yeast vector (CEN/ARS, TRP1)			
pRS315 is a low-copy yeast vector (CEN/ARS, LEU2)			
pRS316 is a low-copy yeast vector (CEN/ARS, URA3)			
pRS424 is a high-copy yeast vector (2-micron, TRP1)			
pRS425 is a high-copy yeast vector (2-micron, LEU2)			
pRS426 is a high-copy yeast vector (2-micron, URA3)			

CONCLUSION

MAP kinase pathway is made up of protein chains from receptor to transcription factors and is involved in almost all aspects of life. Signaling pathways are intricately organized for cells to make the most beneficial decision in the ever changing environment. We are stepping one step closer to understanding the complexity of signaling network with all the advancement in scientific research. However, some basic mechanisms that have been previously difficult to identify needs to be explored for a comprehensive understanding and progression of cell manipulations. The unique design of MAP kinase pathway, the three components or larger signaling cascade, must have evolved for a reason. Since simple one-step process is much more convenient for a straight forward signal delivery, multi-step operation was created probably for regulatory purposes. It seems that it sometime works to diversify itself. As seen from the RPS of isogenic yeast population, diversity is created during the course of signal transduction. Diversity created this way is efficient and always inherent. It is more efficient considering time and space as variations created from signaling pathway does not require genetic changes.

Other times it is tightly controlled with multiple feedback regulations. In every process that transpires in this world, a bottle neck, the rate-determining step exists. From our research we have determined that MAPKKK activation of MAPKK is the rate-determining step. It is also where amplification takes place. However, the freedom to adjust signaling capacity that exists in the beginning of signal transduction is restricted once it goes down to MAPKK and MAPK. Once the signal reaches the final player, tight regulation takes over. It is as if cell knows that after some point it is too late to change minds.

A key is the balance between diversity and reliability. Diversity is what keeps us from going extinct in unpredictable environment, but in signal response a boundary has to be set for a dependable outcome when the environment is peaceful.

REFERENCES

1. Alberts B, J.A., Lewis J, et al. Studying Gene Expression and Function, in *Molecular Biology of the Cell* Vol. 4th edition. (Garland Science, New York; 2002).
2. Kamisaka, Y., Kimura, K., Uemura, H. & Yamaoka, M. Overexpression of the active diacylglycerol acyltransferase variant transforms Saccharomyces cerevisiae into an oleaginous yeast. *Appl Microbiol Biotechnol* **97**, 7345-7355 (2013).
3. Ding, J. *et al.* Acetic acid inhibits nutrient uptake in Saccharomyces cerevisiae: auxotrophy confounds the use of yeast deletion libraries for strain improvement. *Appl Microbiol Biotechnol* **97**, 7405-7416 (2013).
4. Ofiteru, A.M. *et al.* Overexpression of the PHO84 gene causes heavy metal accumulation and induces Ire1p-dependent unfolded protein response in Saccharomyces cerevisiae cells. *Appl Microbiol Biotechnol* **94**, 425-435 (2012).
5. Dohmen, R.J. *et al.* An essential yeast gene encoding a homolog of ubiquitin-activating enzyme. *J Biol Chem* **270**, 18099-18109 (1995).
6. Tong, A.H. *et al.* Systematic genetic analysis with ordered arrays of yeast deletion mutants. *Science* **294**, 2364-2368 (2001).
7. Farabaugh, P.J. Programmed translational frameshifting. *Annu Rev Genet* **30**, 507-528 (1996).
8. Kim, Y.G., Su, L., Maas, S., O'Neill, A. & Rich, A. Specific mutations in a viral RNA pseudoknot drastically change ribosomal frameshifting efficiency. *Proc Natl Acad Sci U S A* **96**, 14234-14239 (1999).
9. Kim, Y.G., Maas, S., Wang, S.C. & Rich, A. Mutational study reveals that tertiary interactions are conserved in ribosomal frameshifting pseudoknots of two luteoviruses. *Rna* **6**, 1157-1165 (2000).
10. Blake, W.J., M, K.A., Cantor, C.R. & Collins, J.J. Noise in eukaryotic gene expression. *Nature* **422**, 633-637 (2003).
11. Spencer, S.L., Gaudet, S., Albeck, J.G., Burke, J.M. & Sorger, P.K. Non-genetic origins of cell-to-cell variability in TRAIL-induced apoptosis. *Nature* **459**, 428-432 (2009).
12. Elion, E.A., Grisafi, P.L. & Fink, G.R. FUS3 encodes a cdc2+/CDC28-related kinase required for the transition from mitosis into conjugation. *Cell* **60**, 649-664 (1990).
13. Hur, J.Y. *et al.* Quantitative profiling of dual phosphorylation of Fus3 MAP kinase in Saccharomyces cerevisiae. *Mol Cells* **26**, 41-47 (2008).
14. Kranz, J.E., Satterberg, B. & Elion, E.A. The MAP kinase Fus3 associates with and phosphorylates the upstream signaling component Ste5. *Genes Dev* **8**, 313-327 (1994).
15. Huh, W.K. *et al.* Global analysis of protein localization in budding yeast. *Nature* **425**, 686-691 (2003).
16. Longtine, M.S. *et al.* Additional modules for versatile and economical PCR-

based gene deletion and modification in Saccharomyces cerevisiae. *Yeast* **14**, 953-961 (1998).
17. Hoffman, G.A., Garrison, T.R. & Dohlman, H.G. Analysis of RGS proteins in Saccharomyces cerevisiae. *Methods Enzymol* **344**, 617-631 (2002).
18. Farabaugh, P.J. Translational frameshifting: Implications for the mechanism of translational frame maintenance, in *Progress in Nucleic Acid Research and Molecular Biology*, Vol. Volume 64 131-170 (Academic Press, 2000).
19. Merlini, L., Dudin, O. & Martin, S.G. Mate and fuse: how yeast cells do it. *Open Biol* **3**, 130008 (2013).
20. Hur, J.Y., Park, M.C., Suh, K.Y. & Park, S.H. Synchronization of cell cycle of Saccharomyces cerevisiae by using a cell chip platform. *Mol Cells* **32**, 483-488 (2011).
21. Schwartz, M.A. & Madhani, H.D. Principles of MAP kinase signaling specificity in Saccharomyces cerevisiae. *Annu Rev Genet* **38**, 725-748 (2004).
22. Murphy, L.O. & Blenis, J. MAPK signal specificity: the right place at the right time. *Trends Biochem Sci* **31**, 268-275 (2006).
23. Boone, C., Bussey, H. & Andrews, B.J. Exploring genetic interactions and networks with yeast. *Nat Rev Genet* **8**, 437-449 (2007).
24. Chong, Y.T. *et al.* Yeast Proteome Dynamics from Single Cell Imaging and Automated Analysis. *Cell* **161**, 1413-1424 (2015).
25. Aigner, A. Applications of RNA interference: current state and prospects for siRNA-based strategies in vivo. *Appl Microbiol Biotechnol* **76**, 9-21 (2007).
26. Nakayashiki, H. & Nguyen, Q.B. RNA interference: roles in fungal biology. *Curr Opin Microbiol* **11**, 494-502 (2008).
27. Eggert, U.S., Field, C.M. & Mitchison, T.J. Small molecules in an RNAi world. *Mol Biosyst* **2**, 93-96 (2006).
28. Ramanathan, C. *et al.* Cell type-specific functions of period genes revealed by novel adipocyte and hepatocyte circadian clock models. *PLoS Genet* **10**, e1004244 (2014).
29. Yang, L. *et al.* Knockdown of PPAR delta gene promotes the growth of colon cancer and reduces the sensitivity to bevacizumab in nude mice model. *PLoS One* **8**, e60715 (2013).
30. Yu, J. *et al.* Transgenic RNAi-mediated reduction of MSY2 in mouse oocytes results in reduced fertility. *Dev Biol* **268**, 195-206 (2004).
31. Elion, E.A., Brill, J.A. & Fink, G.R. FUS3 represses CLN1 and CLN2 and in concert with KSS1 promotes signal transduction. *Proc Natl Acad Sci U S A* **88**, 9392-9396 (1991).
32. Burchett, S.A., Scott, A., Errede, B. & Dohlman, H.G. Identification of novel pheromone-response regulators through systematic overexpression of 120 protein kinases in yeast. *J Biol Chem* **276**, 26472-26478 (2001).
33. Choi, K.Y., Kranz, J.E., Mahanty, S.K., Park, K.S. & Elion, E.A. Characterization of Fus3 localization: active Fus3 localizes in complexes of varying size and specific activity. *Mol Biol Cell* **10**, 1553-1568 (1999).
34. Hilioti, Z. *et al.* Oscillatory phosphorylation of yeast Fus3 MAP kinase

controls periodic gene expression and morphogenesis. *Curr Biol* **18**, 1700-1706 (2008).
35. Bodai, L. & Marsh, J.L. A novel target for Huntington's disease: ERK at the crossroads of signaling. The ERK signaling pathway is implicated in Huntington's disease and its upregulation ameliorates pathology. *Bioessays* **34**, 142-148 (2012).
36. Kim, E.K. & Choi, E.J. Pathological roles of MAPK signaling pathways in human diseases. *Biochim Biophys Acta* **1802**, 396-405 (2010).
37. Bardwell, L. A walk-through of the yeast mating pheromone response pathway. *Peptides* **26**, 339-350 (2005).
38. Mayawala, K., Gelmi, C.A. & Edwards, J.S. MAPK cascade possesses decoupled controllability of signal amplification and duration. *Biophys J* **87**, L01-02 (2004).
39. Shevchenko, A., Tomas, H., Havlis, J., Olsen, J.V. & Mann, M. In-gel digestion for mass spectrometric characterization of proteins and proteomes. *Nat Protoc* **1**, 2856-2860 (2006).
40. Kim, J.K. *et al.* Selective enrichment and mass spectrometric identification of nitrated peptides using fluorinated carbon tags. *Anal Chem* **83**, 157-163 (2011).
41. Shim, E. & Park, S.H. Identification of a novel Ser/Thr protein phosphatase Ppq1 as a negative regulator of mating MAP kinase pathway in Saccharomyces cerevisiae. *Biochem Biophys Res Commun* **443**, 252-258 (2014).
42. Andrusiak, M.G. & Jin, Y. Context Specificity of Stress-activated Mitogen-activated Protein (MAP) Kinase Signaling: The Story as Told by Caenorhabditis elegans. *J Biol Chem* **291**, 7796-7804 (2016).
43. Lee, Y., Kim, Y.J., Kim, M.H. & Kwak, J.M. MAPK Cascades in Guard Cell Signal Transduction. *Front Plant Sci* **7**, 80 (2016).
44. Rattanasinchai, C. & Gallo, K.A. MLK3 Signaling in Cancer Invasion. *Cancers (Basel)* **8** (2016).
45. Furukawa, K. & Hohmann, S. A fungicide-responsive kinase as a tool for synthetic cell fate regulation. *Nucleic Acids Res* **43**, 7162-7170 (2015).
46. Kang, H.B. *et al.* Metabolic Rewiring by Oncogenic BRAF V600E Links Ketogenesis Pathway to BRAF-MEK1 Signaling. *Mol Cell* **59**, 345-358 (2015).
47. Martin, H. *et al.* Differential genetic interactions of yeast stress response MAPK pathways. *Mol Syst Biol* **11**, 800 (2015).
48. Cardinale, B.J. *et al.* Biodiversity loss and its impact on humanity. *Nature* **486**, 59-67 (2012).
49. Tsimring, L.S. Noise in biology. *Rep Prog Phys* **77**, 026601 (2014).
50. Spudich, J.L. & Koshland Jr, D. Non-genetic individuality: chance in the single cell. *Nature* **262**, 467-471 (1976).
51. Hughes, A.R., Inouye, B.D., Johnson, M.T., Underwood, N. & Vellend, M. Ecological consequences of genetic diversity. *Ecol Lett* **11**, 609-623 (2008).
52. Loreau, M. *et al.* Biodiversity and ecosystem functioning: current

knowledge and future challenges. *science* **294**, 804-808 (2001).
53. Torres-Padilla, M.-E. & Chambers, I. Transcription factor heterogeneity in pluripotent stem cells: a stochastic advantage. *Development* **141**, 2173-2181 (2014).
54. Kærn, M., Elston, T.C., Blake, W.J. & Collins, J.J. Stochasticity in gene expression: from theories to phenotypes. *Nat Rev Genet* **6**, 451-464 (2005).
55. Elowitz, M.B., Levine, A.J., Siggia, E.D. & Swain, P.S. Stochastic gene expression in a single cell. *Science* **297**, 1183-1186 (2002).
56. Huang, S. Non-genetic heterogeneity of cells in development: more than just noise. *Development* **136**, 3853-3862 (2009).
57. Eldar, A. & Elowitz, M.B. Functional roles for noise in genetic circuits. *Nature* **467**, 167-173 (2010).
58. Swain, P.S., Elowitz, M.B. & Siggia, E.D. Intrinsic and extrinsic contributions to stochasticity in gene expression. *Proc Natl Acad Sci USA* **99**, 12795-12800 (2002).
59. Novick, A. & Weiner, M. Enzyme induction as an all-or-none phenomenon. *Proc Natl Acad Sci USA* **43**, 553-566 (1957).
60. Rhee, A., Cheong, R. & Levchenko, A. Noise decomposition of intracellular biochemical signaling networks using nonequivalent reporters. *Proc Natl Acad Sci USA* **111**, 17330-17335 (2014).
61. Cheong, R., Rhee, A., Wang, C.J., Nemenman, I. & Levchenko, A. Information transduction capacity of noisy biochemical signaling networks. *Science* **334**, 354-358 (2011).
62. Kiviet, D.J. *et al.* Stochasticity of metabolism and growth at the single-cell level. *Nature* **514**, 376-379 (2014).
63. McAdams, H.H. & Arkin, A. Stochastic mechanisms in gene expression. *Proc Natl Acad Sci USA* **94**, 814-819 (1997).
64. Colman-Lerner, A. *et al.* Regulated cell-to-cell variation in a cell-fate decision system. *Nature* **437**, 699-706 (2005).
65. Levchenko, A. & Nemenman, I. Cellular noise and information transmission. *Curr Opin Biotechnol* **28**, 156-164 (2014).
66. Levine, J.H., Lin, Y. & Elowitz, M.B. Functional roles of pulsing in genetic circuits. *Science* **342**, 1193-1200 (2013).
67. Sanchez, A. & Golding, I. Genetic determinants and cellular constraints in noisy gene expression. *Science* **342**, 1188-1193 (2013).
68. Sherman, M.S., Lorenz, K., Lanier, M.H. & Cohen, B.A. Cell-to-cell variability in the propensity to transcribe explains correlated fluctuations in gene expression. *Cell Syst* **1**, 315-325 (2015).
69. Raser, J.M. & O'Shea, E.K. Control of stochasticity in eukaryotic gene expression. *Science* **304**, 1811-1814 (2004).
70. Wang, Z. & Zhang, J. Impact of gene expression noise on organismal fitness and the efficacy of natural selection. *Proc Natl Acad Sci USA* **108**, E67-76 (2011).
71. Raj, A. & van Oudenaarden, A. Nature, nurture, or chance: stochastic gene expression and its consequences. *Cell* **135**, 216-226 (2008).

72. Shahrezaei, V. & Marguerat, S. Connecting growth with gene expression: of noise and numbers. *Curr Opin Microbiol* **25**, 127-135 (2015).
73. Duina, A.A., Miller, M.E. & Keeney, J.B. Budding yeast for budding geneticists: a primer on the Saccharomyces cerevisiae model system. *Genetics* **197**, 33-48 (2014).
74. Ratcliff, W.C., Fankhauser, J.D., Rogers, D.W., Greig, D. & Travisano, M. Origins of multicellular evolvability in snowflake yeast. *Nat Commun* **6**, 6102 (2015).
75. Rossouw, D., Bagheri, B., Setati, M.E. & Bauer, F.F. Co-Flocculation of Yeast Species, a New Mechanism to Govern Population Dynamics in Microbial Ecosystems. *PLoS One* **10**, e0136249 (2015).
76. Rogers, D.W. & Greig, D. Experimental evolution of a sexually selected display in yeast. *Proc Biol Sci* **276**, 543-549 (2009).
77. Jackson, C.L. & Hartwell, L.H. Courtship in S. cerevisiae: both cell types choose mating partners by responding to the strongest pheromone signal. *Cell* **63**, 1039-1051 (1990).
78. Sheff, M.A. & Thorn, K.S. Optimized cassettes for fluorescent protein tagging in Saccharomyces cerevisiae. *Yeast* **21**, 661-670 (2004).
79. Mumberg, D., Muller, R. & Funk, M. Yeast vectors for the controlled expression of heterologous proteins in different genetic backgrounds. *Gene* **156**, 119-122 (1995).
80. Park, M.C., Hur, J.Y., Kwon, K.W., Park, S.H. & Suh, K.Y. Pumpless, selective docking of yeast cells inside a microfluidic channel induced by receding meniscus. *Lab Chip* **6**, 988-994 (2006).
81. Ryu, J. & Park, S.H. Simple synthetic protein scaffolds can create adjustable artificial MAPK circuits in yeast and mammalian cells. *Sci Signal* **8**, ra66 (2015).
82. Park, M.C., Hur, J.Y., Cho, H.S., Park, S.H. & Suh, K.Y. High-throughput single-cell quantification using simple microwell-based cell docking and programmable time-course live-cell imaging. *Lab Chip* **11**, 79-86 (2011).
83. Hur, J.Y., Park, M.C., Suh, K.-Y. & Park, S.-H. Synchronization of cell cycle of Saccharomyces cerevisiae by using a cell chip platform. *Mol Cells* **32**, 483-488 (2011).
84. Pedrali-Noy, G. *et al.* Synchronization of HeLa cell cultures by inhibition of DNA polymerase alpha with aphidicolin. *Nucleic Acids Res* **8**, 377-387 (1980).
85. Herskowitz, I. Life cycle of the budding yeast Saccharomyces cerevisiae. *Microbiol Rev* **52**, 536-553 (1988).
86. Hennig, S., Clemens, A., Rodel, G. & Ostermann, K. A yeast pheromone-based inter-species communication system. *Appl Microbiol Biotechnol* **99**, 1299-1308 (2015).
87. Severin, F.F. & Hyman, A.A. Pheromone induces programmed cell death in S. cerevisiae. *Curr Biol* **12**, R233-235 (2002).
88. Dohlman, H.G. & Thorner, J.W. Regulation of G protein-initiated signal transduction in yeast: paradigms and principles. *Annu Rev Biochem* **70**,

703-754 (2001).
89. Sacristan-Reviriego, A., Martin, H. & Molina, M. Identification of putative negative regulators of yeast signaling through a screening for protein phosphatases acting on cell wall integrity and mating MAPK pathways. *Fungal Genet Biol* **77**, 1-11 (2015).
90. Sanchez, A., Choubey, S. & Kondev, J. Stochastic models of transcription: from single molecules to single cells. *Methods* **62**, 13-25 (2013).
91. Raser, J.M. & O'Shea, E.K. Noise in gene expression: origins, consequences, and control. *Science* **309**, 2010-2013 (2005).
92. Woods, H.A. Mosaic physiology from developmental noise: within-organism physiological diversity as an alternative to phenotypic plasticity and phenotypic flexibility. *J Exp Biol* **217**, 35-45 (2014).
93. Frydlova, I., Basler, M., Vasicova, P., Malcova, I. & Hasek, J. Special type of pheromone-induced invasive growth in Saccharomyces cerevisiae. *Curr Genet* **52**, 87-95 (2007).
94. Hao, N. *et al.* Regulation of cell signaling dynamics by the protein kinase-scaffold Ste5. *Molecular cell* **30**, 649-656 (2008).
95. Malleshaiah, M.K., Shahrezaei, V., Swain, P.S. & Michnick, S.W. The scaffold protein Ste5 directly controls a switch-like mating decision in yeast. *Nature* **465**, 101-105 (2010).
96. Paliwal, S. *et al.* MAPK-mediated bimodal gene expression and adaptive gradient sensing in yeast. *Nature* **446**, 46-51 (2007).
97. Nishant, K.T. *et al.* The baker's yeast diploid genome is remarkably stable in vegetative growth and meiosis. *PLoS Genet* **6**, e1001109 (2010).
98. Booth, I.R. Stress and the single cell: intrapopulation diversity is a mechanism to ensure survival upon exposure to stress. *Int J Food Microbiol* **78**, 19-30 (2002).
99. Zechner, C. & Koeppl, H. Uncoupled analysis of stochastic reaction networks in fluctuating environments. *PLoS Comput Biol* **10**, e1003942 (2014).
100. Tabbaa, O.P., Nudelman, G., Sealfon, S.C., Hayot, F. & Jayaprakash, C. Noise propagation through extracellular signaling leads to fluctuations in gene expression. *BMC Syst Biol* **7**, 94 (2013).
101. Thattai, M. & van Oudenaarden, A. Stochastic gene expression in fluctuating environments. *Genetics* **167**, 523-530 (2004).
102. Levin, B.R. Microbiology. Noninherited resistance to antibiotics. *Science* **305**, 1578-1579 (2004).
103. Levin, B.R. & Rozen, D.E. Non-inherited antibiotic resistance. *Nat Rev Microbiol* **4**, 556-562 (2006).
104. El Meouche, I., Siu, Y. & Dunlop, M.J. Stochastic expression of a multiple antibiotic resistance activator confers transient resistance in single cells. *Sci Rep* **6**, 19538 (2016).

ABSTRACT IN KOREAN
국문 초록

MAP kinase 신호전달계의 피드백 조절 기작과 속도 결정 단계 연구

세포의 연구에서 신호 전달 네트워트는 활발한 연구 대상이 되어 왔음에도 불구하고 몇 가지 필수적인 정보들이 여전히 알려지지 않은 상태이다. 단백질 복합체 조절에 있어 피드백 제어의 체계와 속도 결정 단계를 파악하는 것은 신호전달 체계를 정확히 판단하는데 매우 중요하다. 세포 신호 전달의 조절 체계를 이해하기 위해서, 우리는 효모의 짝짓기 신호 전달 과정을 모델로 선정하였다. 이성의 페로몬에 의해 자극을 받으면 효모는 Ste11, Ste7 과 Fu3 로 구성된 신호전달체계를 통해 신호를 전달한다. 이들 세가지 구성요소의 양을 조절하면서 그들이 신호전달체계의 능력에 미치는 영향을 관찰해 본 결과 Ste11 이 가장 큰 영향력을 가진 요소임을 알 수 있었다. 또한 수학적 모형 제작을 통해 실험 결과를 설명할 수 있는 핵심 구조와 최상의 구조를 찾을 수 있었다. 최상의 구조는 하나의 양성 피드백과 두개의 음성 피드백을 가진 구조로 밝혀졌고, 양성 피드백의 신호의 증폭을 일으키며 음성 피드백은 신호를 제한하는 역할을 하는 것으로 보인다. 또한 기존에 알려지지 않은 Ppq1 을 통한 음성 피드백을 발견하였다. 짝짓기 신호 전달에 의존하는 Ppq1 은 Ste7 의 탈인산화 효소로 작용하며 음성적으로 신호전달체계를 조절하는 것으로 보인다.

한편, 짝짓기 신호 전달 반응은 같은 유전자적 배경과 환경에 있음에도 다양성을 보이는데, 이것이 단순한 부작용이 아닌 동일한

생물체들의 다양성을 증가시켜주는 하나의 체계임을 확인하였다. 이러한 특이성은 모든 세포가 가지고 있고 후대에도 다양성 그대로 전달이 되는데, 이는 내재된 다양성이라 할 수 있다. 이를 통해 효모세포 한 개는 다양한 반응을 보일 수 있는 잠재력을 갖게 되고 효모개체군으로 보면 다양한 반응이 나타나게 되는 동시에 개체군의 평균으로 보면 같은 신호에는 항상 일정한 반응을 보여 다양성과 신뢰성을 동시에 이룰 수 있게 된다.

MAPK 신호 전달 체계는 진핵 생물계에서 잘 보존되어 있으며 세포 안의 여러 가지 신호 전달을 매개하기 때문에 매우 중요하다. 본 연구를 시작으로, 다른 신호를 담당하거나 다른 종에 존재하는 신호 전달계에 이와 같은 조절 기작이 존재하는지 알아보는 것과 이를 이용해 합성 생물학에 응용해보는 것이 매우 의미있는 연구가 될 것이라고 생각된다.

주요어: 다양성, 단백질 발현량, 속도결정단계, 신호 반응 프로파일, 피드백 조절 기작, 효모
학번: 2009-30859